



Since January 2020 Elsevier has created a COVID-19 resource centre with free information in English and Mandarin on the novel coronavirus COVID-19. The COVID-19 resource centre is hosted on Elsevier Connect, the company's public news and information website.

Elsevier hereby grants permission to make all its COVID-19-related research that is available on the COVID-19 resource centre - including this research content - immediately available in PubMed Central and other publicly funded repositories, such as the WHO COVID database with rights for unrestricted research re-use and analyses in any form or by any means with acknowledgement of the original source. These permissions are granted for free by Elsevier for as long as the COVID-19 resource centre remains active.



## Letters to the Editor

***Neisseria meningitidis* carriage in indigenous peoples of Amazonas State, Brazil**

Dear Editor,

In this Journal, Basta and colleagues recently reported rates of meningococcal carriage within households in the African meningitis belt.<sup>1</sup> We report the results of an investigation of *Neisseria meningitidis* carriage in indigenous communities with different contact patterns with non-indigenous in the state of Amazonas, Brazil. A feature of the nature of this bacterium is its transmission from person to person, which normally results in asymptomatic pharyngeal carriage, and progression to disease is an exception.<sup>2</sup> Indigenous peoples are at higher risk for invasive diseases caused by encapsulated bacteria such as *N. meningitidis* compared to other population.<sup>3</sup> Meningococcal disease is a serious threat for indigenous people living in the state of Amazonas, where there is insufficient epidemiological information to optimize the planning and implementation of interventions.<sup>4,5</sup>

A cross-sectional meningococcal carriage study in three different indigenous ethnic groups – i.e., Mura, Munduruku, and Mura-Pirahã – located near the course of Madeira River in the state of Amazonas, Brazil, was carried out in 2016 and 2017 (Fig. 1).

The study was approved by the National Commission for Research Ethics (CONEP) of the Ministry of Health (protocol 1.351.186) and the local Indigenous Council. Surveillance data of meningococcal disease was obtained from the Indigenous Special Sanitary District (DSEI) of Manaus and the Amazonas State Department of Health.

The indigenous villages were visited prior to the meningococcal carriage investigation for a survey of the number of inhabitants and the presentation of the study to the leaders. Demographic data, antibiotic use within the last month, alcohol consumption, and smoking were obtained from each individual enrolled, as well as consent for participation. Vaccine status was obtained from individual vaccination booklet or indigenous health records. The number of persons per house was obtained with the chief of the family group. The housing models in each village are presented in Fig. 2.

The Mura (access by road or waterway) and the Munduruku (access by waterway) communities are located less than 30 km from the nearest city, with daily or regular displacement of indigenous and without restriction or sporadic entry of non-indigenous into the village, respectively. The Mura-Pirahã live in a remote area (access by waterway) located about 140 km from the nearest city, and contact with other people is sporadic and usually occurs outside the village (Fig. 1).

Altogether, 586 individuals aged 1 month to 96 years were examined with throat swabs by a single investigator (Table 1). Samples were taken with Rayon swabs (per-oral) from the posterior

pharyngeal wall with direct plating onto blood agar plates containing VCNT (Oxoid, Basingstoke, Hampshire, UK) in the field, and the inoculums were immediately streaked with disposable loops for isolated colonies. The plates were transported in containers with CO<sub>2</sub> atmosphere to the hospital laboratory at the nearest city within 6–8 h of collection, before being transported to the capital city of Manaus after overnight culture.

Suspected colonies were subcultured, and bacteria growth with the appearance of Gram-negative diplococcus and a positive oxidase test were identified using api NH (bioMérieux, Marcy-l'Étoile, France). Serogroup was determined by slide agglutination with specific rabbit antisera (BD Difco, Maryland, USA). The genetic lineage of *N. meningitidis* was determined by multilocus sequence typing (MLST).<sup>6</sup> Sequence types (STs) and alleles at antigenic loci were assigned by the *N. meningitidis* MLST database (<http://www.pubmlst.org/neisseria>).

A bivariate analysis was performed by using Epi Info™ (version 3.5.4, Centers for Disease Control and Prevention, Atlanta, GA, USA). Differences between groups were assessed using chi-square tests with Yates's correction or where appropriate, Fisher's exact test.

The surveillance system recorded two suspected cases of meningococcal disease in Mura and Munduruku children in 2014 and 2015, respectively; both cases had a hemorrhagic rash and died at presentation or following hospital admission.

Demographic data, number of participants, and meningococcal vaccine status are presented in Table 1. The use of antibiotics in the last month was reported by 13 Mura and 17 Munduruku.

The frequency of *N. meningitidis* asymptomatic infection in each ethnic group is shown in Table 2. Carriage ratio was 1.9% (11/586) and the age of carriers ranged from 10 to 33 years; mostly was 10 to 19 years (73%; 8/11). There was no statistically significant difference in the prevalence of carriers between men (2.7%; 8/293) and women (1%; 3/293) ( $P=0.1$ ). It was not found a risk factor for carriage with *N. meningitidis* at the individual level. Nonetheless, all carriers reported frequent displacement to the nearest city.

*N. meningitidis* isolates were characterized as serogroup B. These isolates were assigned to ST-13110 (-), ST-13111 (cc1136), which were novel, and ST-11406 (-). The ST-13110 was isolated only from Munduruku carriers and ST-11406 from a single Mura carrier. The ST-13111 is a single-locus variant of ST-1136 that differs at *fumC*, which was found in the three ethnic groups.

The rates of meningococcal carriage in teenagers observed in this study are in line with studies done in other geographical regions.<sup>2</sup> Carriage prevalence differences were not statically significant among the three ethnic groups. Also, a risk factor for a positive infection was not established, probably due to the small number of carriers. A factor that may have affected carriage prevalence was the loss of participants and the difficult field conditions. Thus, the carriage prevalence could be higher than estimated here.

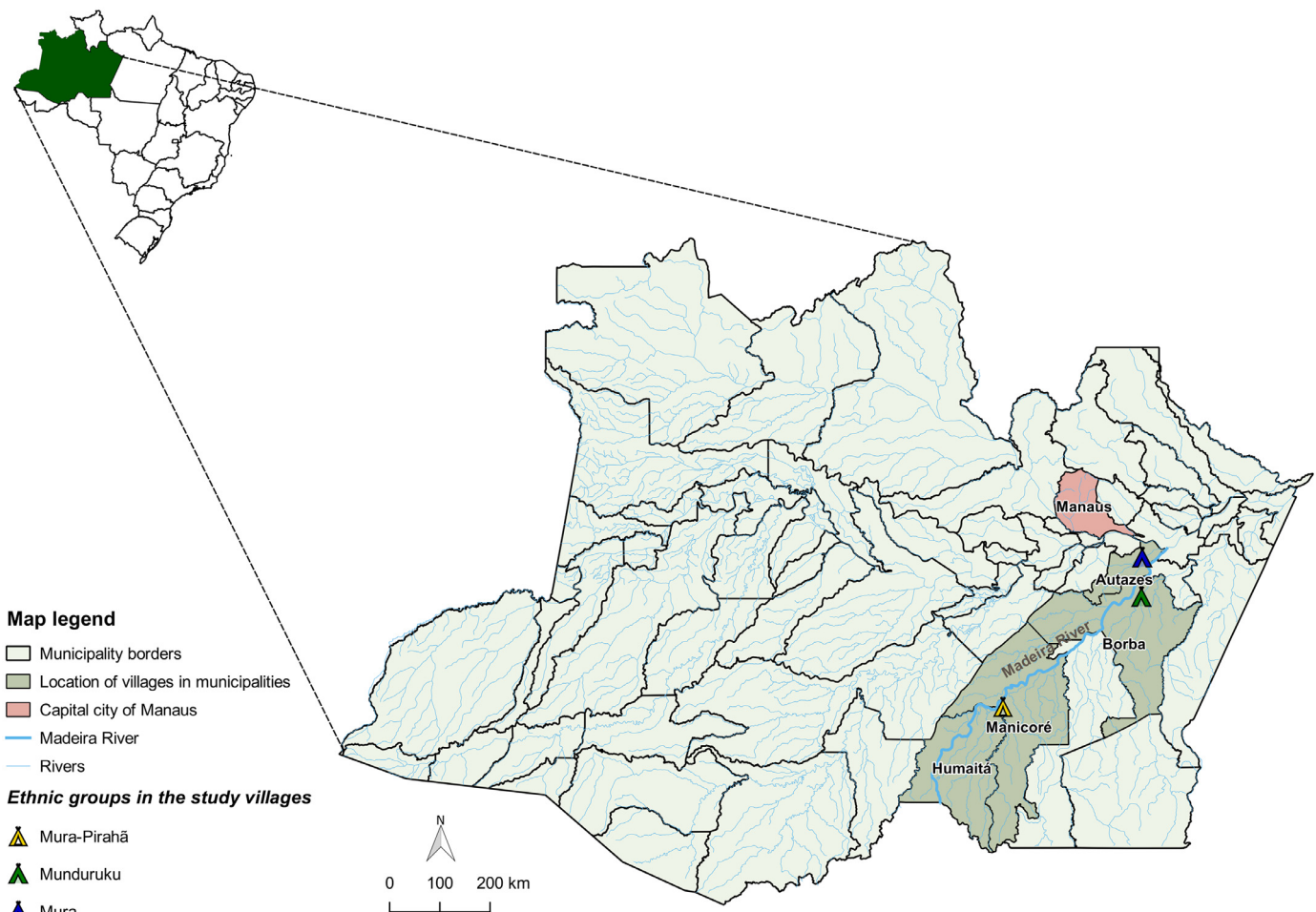


Fig. 1. Geographical localization of the indigenous villages investigated in the study.

Table 1

Demographic data, number of exams performed, and meningococcal vaccine status of indigenous included in the study.

	Total (n = 702)	Mura (n = 260)	Munduruku (n = 270)	Mura-Pirahã (n = 172)
Male	355 (51%)	127 (49%)	135 (50%)	93 (54%)
Female	347 (49%)	133 (51%)	135 (50%)	79 (46%)
Age				
< 1	22 (3%)	10 (4%)	3 (1%)	9 (5%)
1–10	234 (34%)	68 (26%)	93 (34%)	73 (42%)
11–20	169 (24%)	65 (25%)	77 (29%)	27 (16%)
21–50	219 (31%)	93 (36%)	77 (29%)	49 (29%)
>50	58 (8%)	24 (9%)	20 (7%)	14 (8%)
N° of people examined with throat swabs	586 (83%)	210 (81%)	268 (99%)	108 (63%)
Vaccinees with MCC–CRM <sub>197</sub>	72 (10%)	16 (9%) <sup>Δ</sup>	1 (0,4%) <sup>▲</sup>	55 (32%) <sup>□</sup>

<sup>Δ</sup>(All individuals < 13 years old); <sup>▲</sup>(3 years old); <sup>□</sup>(All individuals < 8 years old).

The genus *Neisseria* was shown to be common in the oral microbiota of Amazon Amerindians in Venezuela.<sup>7</sup> However, meningococcal carriage investigation had not been performed prior to this study on indigenous people of Amazonas State, Brazil. There was a single carriage study conducted in Amazonas State, which investigated riverside people.<sup>5</sup> The carriage prevalence of *N. meningitidis* in the villagers was 3% (2/79) and the majority (67%) of carriers was over 10 years older.

The coverage with MCC–CRM<sub>197</sub> vaccine was low and it should not have had any influence in the fact that no serogroup C was found. Indeed, serogroup C *N. meningitidis* is rarely found in carriers or establish a carrier state of short duration.<sup>8,9</sup>

Molecular typing demonstrated a few clones causing subclinical infection in all three ethnic groups. The ST-11406 and ST-13110

are singleton unrelated to other isolates in the database. The ST-13111 belongs to ST-1136 clonal complex with STs normally recovered from carriers.<sup>10</sup> Nevertheless, isolates that were not assigned to a known clonal complex may cause invasive disease,<sup>8</sup> as is the case with ST-11406.<sup>4</sup>

We demonstrated *N. meningitidis* carriage among indigenous people investigated in this study, which suggested the pattern of late acquisition in childhood. Indigenous people in the state of Amazonas do not have access to basic health care or this is not easy when needed, with tragic consequences of delayed treatment of medical emergencies. Therefore, the true burden of meningococcal disease in indigenous people must be underestimated. Take into account the downhill course of meningococcal disease and the constraint of indigenous to access hospital care,

## 1. Mura



## 2. Munduruku



## 3. Mura-Pirahã



Fig. 2. Housing models in the indigenous villages of the study: Mura (1), Munduruku (2), and Mura-Pirahã (3).

Table 2

Prevalence of *Neisseria meningitidis* carriage among 586 indigenous from 3 different ethnic groups and laboratory analysis of nasopharynx isolates.

Carriers	Age (years)	Serogroup	Sequence type	Clonal complex
2,4% (5/210)	Mura (M)			
M16/7 (male)	33	B	11406	(-)
M17/6 (female)	13	B	13111	1136
M29/4 (female)	10	B	13111	1136
M50/3 (female)	18	B	13111	1136
M50/4 (male)	16	B	13111	1136
1,5% (4/268)	Munduruku (MK)			
MK2/3 (male)	15	B	13110	(-)
MK4/5 (female)	19	B	13111	1136
MK10/5 (male)	17	B	13110	(-)
MK13/10 (male)	25	B	13110	(-)
1,8% (2/108)	Mura-Pirahã (MP)			
MP13 (male)	29	B	13111	1136
MP70 (male)	14	B	13111	1136
1,9% (11/586)	Total			

immunization should be expanded with vaccines covering the most common serogroups associated with invasive disease.

#### Declaration of Competing Interest

The authors declare no conflicts of interest.

#### Funding

Dr. Lima was supported by the [Foundation for Research Support of the State of Amazonas \(FAPEAM\)](#) with a doctoral grant (17282.410.13664.10092013).

#### Acknowledgments

We cannot thank enough all indigenous people involved in this study, in particular Ilair Pereira dos Santos (Mura), Kleuton Lopes de Matos (Munduruku), and Caissô (Mura-Pirahã). We acknowledge the help of the health professionals of the Indigenous Special Sanitary District (DSEI) of Manaus and the staff of the Indigenous Regional Office Kwatã/Laranjal, Indigenous National Foundation (FUNAI), for help with data collection, cooperation, and support. We are thanked with staff of the Amazonas State Department of Health. We thank Fernanda R. Fonseca of the Geoprocessing Core/ILMD/FIOCRUZ for the digital map. We also thank Mrs. Vilma dos Santos of the LESM/IOC/FIOCRUZ and Mrs. Juracy Aquino de Souza of the ILMD/FIOCRUZ for the laboratory technical support. This publication made use of the *Neisseria* Multi Locus Sequence Typing website (<https://pubmlst.org/neisseria/>) developed by Keith Jolley and sited at the University of Oxford (Jolley & Maiden 2010, *BMC Bioinformatics*, 11:595).

#### References

- Basta N.E., Berthe A., Keita M., Onwuchekwa U., Tamboura B., Traore A., et al. Meningococcal carriage within households in the African meningitis belt: a longitudinal pilot study. *J Infection* 2018;**76**:140–8.
- Trotter C.L., Gay N.J., Edmunds W.J.. Dynamic models of meningococcal carriage, disease, and the impact of serogroup C conjugate vaccination. *Am J Epidemiol* 2005;**162**:89–100.
- Butler J.C., Crengle S., Cheek J.E., Leach A.J., Lennon D., O'Brien K.L., et al. Emerging infectious diseases among indigenous peoples. *Emerg Infect Dis* 2001;**7**(3 Suppl):554–5.
- Silva L.A., Coronato B., Schlackman J., Marsh J.W., Ezeonwuka C., Fernandes A.C.L., et al. *Neisseria meningitidis* disease-associated clones in Amazonas State, Brazil. *Infect Dis* 2018;**50**:697–704.
- Barroso D.E., Silva L.A.. *Neisseria meningitidis*: a neglected cause of infectious haemorrhagic fever in the amazon rainforest. *Braz J Infect Dis* 2007;**11**: 598–602.

6. Maiden M.C., Bygraves J.A., Feil E., Morelli G., Russell J.E., Urwin R., et al. Multilocus sequence typing: a portable approach to the identification of clones within populations of pathogenic microorganisms. *Proc Natl Acad Sci USA* 1998;**95**:3140–5.
7. Contreras M., Costello E.K., Hidalgo G., Magris M., Knight R., Dominguez-Bello M.G.. The bacterial microbiota in the oral mucosa of rural Amerindians. *Microbiology* 2010;**156**:3282–7.
8. Caugant D.A., Tzanakaki G., Kriz P. Lessons from meningococcal carriage studies. *FEMS Microbiol Rev* 2007;**31**:52–63.
9. Claus H., Maiden M.C., Wilson D.J., McCarthy N.D., Jolley K.A., Urwin R., et al. Genetic analysis of meningococci carried by children and young adults. *J Infect Dis* 2005;**191**:1263–71.
10. Ambrosio L., Neri A., Fazio C., Rossolini G.M., Vacca P., Riccobono E., et al. Genomic analysis of *Neisseria meningitidis* carriage isolates during an outbreak of serogroup C clonal complex 11, Tuscany, Italy. *PLoS ONE* 2019;**14**:e0217500.

Kátia M.S. Lima

Laboratory of Microbial Diversity of Importance to Health, Leônidas & Maria Deane Institute, FIOCRUZ, Manaus, AM Brazil

Andréia C.L. Fernandes, Filipe A. Carvalho-Costa, David E. Barroso\*  
Laboratory of Epidemiology and Molecular Systematics, Oswaldo Cruz Institute, FIOCRUZ, Rio de Janeiro, RJ, Brazil

\*Corresponding author at: Laboratory of Epidemiology and Molecular Systematics, Oswaldo Cruz Institute, Av. Brasil 4365, Bldg. 26, Rm. 308, 21040-900 Rio de Janeiro, RJ, Brazil  
E-mail address: barroso@ioc.fiocruz.br (D.E. Barroso)

Accepted 31 January 2020  
Available online 6 February 2020

<https://doi.org/10.1016/j.jinf.2020.01.022>

© 2020 The British Infection Association. Published by Elsevier Ltd. All rights reserved.

## High heart rate at admission as a predictive factor of mortality in hospitalized patients with Lassa fever: An observational cohort study in Sierra Leone



Dear Editor,

Wauquier et al., in the Journal, shown that heart rate level greater than 110bpm at hospital admission for Lassa Fever (LF) is an independent predictive factor associated with a 3.6-fold increased risk of mortality. An estimated 100,000 to 300,000 infections of Lassa fever occur annually, with approximately 5000 deaths, mainly in West Africa.<sup>1,2</sup> Despite this high annual mortality rate, LF has been largely underappreciated regarding its contribution to the overall burden of microbial infections, and particularly in Sierra Leone.

To date only a limited number of late indicators of the clinical outcome are described, such as bleeding, or neurological manifestations.<sup>3,4</sup> It was demonstrated that a rapid evaluation of the clinical outcome and risk of failure detection on clinical presentation can significantly reduce the mortality rate. For that, the search and discovery of new biomarkers that are easily and rapidly accessible become necessary for LF.

We here conducted a retrospective cohort study in confirmed 79 LASV-infected patients admitted on the LF ward at the Kenema Government Hospital (Kenema, Sierra Leone). A Real-Time Reverse Transcription Polymerase Chain Reaction (RT-PCR) was performed to confirm LASV infection, as described.<sup>5</sup> From admission to discharge, 38 clinical symptoms, including clinical hemorrhagic signs and nineteen laboratory test results (including basic metabolic panel, complete blood count, and liver function tests)

were routinely monitored and compiled into a protected database which was used for this study (Table 1).

The final outcome was known for all patients, with an overall case-fatality rate of 53% [95%CI, 0.42–0.64] (42 of the 79 patients), close to that previously observed in Sierra Leone.<sup>6</sup> The estimated median of time to death after the LF onset was about 14 days (95%CI, 11–18), and only 2 days [2–5] after admission to the hospital. However, the median time to death with no significant difference of the delay between the LF onset and admission among the deceased and the survivors. Contrary to our expectations, age and treatment by Ribavirin or other drugs showed no association with the LF outcome (Table 1).

In an univariate analysis LF outcome was only significantly associated with blood urea nitrogen (OR = 1.13 [1.04; 1.28], creatinine (>177 μmol/l, OR=7.5 [1.67; 53.9]) and total bilirubin (OR = 1.09 [1.03; 1.18]) that are biomarkers for kidney function (Table 1). Furthermore, association with serum alanine aminotransferase (OR = 1.002 [1.001; 1.003]) is consistent with known liver malfunction in acute LF, and serum electrolyte perturbations, and more particularly potassium (OR = 1.97 [1.21; 3.63]), can occur through multiple mechanisms and are associated with systemic disease and increased mortality and particularly with heart disease (Table 1). Consistently, the LF outcome was also mostly associated with the heart rate (OR = 1.03 [1.01; 1.05]) (Table 1 and Fig. 1(A)). Multivariate analysis revealed however that only the heart rate remained significant. By the estimation of Youden's maximum,<sup>7</sup> 110bpm was the cut-off (Fig. 1(B)); a heart rate higher than 110bpm increased the risk of mortality by 3.6 times (OR = 3.61 [1.35; 10.22]) with an AUC = 0.68 [95%CI, 0.55–0.80]) (Fig. 1(C)). Finally, the longitudinal evolution of the heart rate graphically reveals differences between the patients who died and survivors during the first ten days of the follow-up (Fig. 1(D)), suggesting that recovery of the normal heart rate is crucial for survival to LASV infection.

Elevated heart rate is associated with cellular signaling events leading to vascular endothelial dysfunction, which is a hallmark of hemorrhagic fevers; previously reported in Ebola virus-infected patients,<sup>8</sup> and strongly associated with severe disease in children with Crimean-Congo hemorrhagic fever.<sup>9</sup>

Our observations are limited by the small sample size, study-site nature, and geographic origin; changes in the genome diversity of the viruses are associated with the spread of LF.<sup>10</sup> Despite these limitations, the measurement of the resting heart rate is an easily accessible clinical parameter that should be used routinely. This conveniently acquired marker has the potential to identify patients with increased fatality risk at the time of admission and could represent an opportunity to clinically assess the effectiveness of in-hospital treatment of patients.

## Declaration of Competing Interest

Dr. Wauquier served as consultant to Metabiota. Drs Gonzalez and Fair were employed by Metabiota. The other authors have declared no conflicts of interest.

## Funding

This work was supported by grant funding by the French National Agency of Research (ANR-13-BSV-0004). The funding agency had no role in study design, data collection and analysis, decision to publish, or preparation of the manuscript.

**Table 1**  
Univariable analysis of patient characteristics at admission according to the Lassa fever outcome.

	Overall	Survived	Died	Normal range	Missing	OR	[95% CI]	<i>p</i>
<b>Outcome</b>	79	37 (47)	42 (53)		0			
<b>Sociodemographics</b>								
Gender					0			
Man	31 (39)	14 (38)	17 (40.5)					
Woman	48 (61)	23 (57)	25 (40.5)			0.67	[0.25; 1.72]	0.41
Pregnant	10 (13)	2 (5)	8 (19)			3.29	[0.69; 24.25]	0.17
Age (years)	22 [14; 30]	20 [13; 32]	22.5 [15.5; 28]		0	0.99	[0.95; 1.02]	0.36
Age (WHO classification)								
0–14 years	20 (25)	10 (27)	10 (24)					
15–24 years	27 (34)	14 (38)	13 (31)			0.93	[0.29; 2.97]	0.90
25 years and more	32 (41)	13 (35)	19 (45)			1.46	[0.47; 4.57]	0.51
Delay between first symptoms and presentation (days)	8 [6; 11]	8 [6; 11]	7 [6; 11]		10 (13)	0.81	[0.29; 2.26]	0.69
<b>Treatments at presentation</b>								
Ribavirin	61 (85)	29 (81)	32 (89)		7 (9)	1.93	[0.53; 8.01]	0.33
Antibiotics	52 (71)	28 (78)	24 (65)		6 (8)	0.53	[0.18; 1.47]	0.23
Antimalarials	7 (10)	4 (11)	3 (9)		8 (10)	0.80	[0.15; 3.90]	0.78
Other medicines	45 (62)	19 (56)	26 (67)		6 (8)	1.58	[0.61; 4.13]	0.35
<b>Vital signs at presentation</b>								
Respiratory Rate (c/min)	28 [24; 33]	26 [24; 32]	28 [26; 36]	12–20	8 (10)	1.04	[0.99; 1.12]	0.17
Systolic blood pressure (mm Hg) (*)	100 [90; 120]	100 [90; 120]	100 [90; 110]	<120	18 (23)	0.31	[0.03; 2.71]	0.30
Diastolic blood pressure (mm Hg) (*)	60 [50; 70]	60 [60; 70]	60 [40; 70]	<80	18 (23)	0.12	[0.01; 0.90]	0.049
Heart Rate (bpm)	98 [86; 118]	84 [71; 99]	111 [90; 135]	60–100	8 (10)	1.03	[1.01; 1.05]	<b>0.009</b>
Temperature (°C)	38.0 [37.0; 38.8]	38.3 [36.0; 38.9]	37.8 [36.9; 38.6]	36.1–37.2	8 (10)	0.74	[0.49; 1.08]	0.12
<b>Laboratory tests</b>								
<b>Basic metabolic</b>								
Blood Urea Nitrogen (mmol/L)	7.9 [3.7; 19.5]	4.4 [3.3; 7.9]	11.9 [6.6; 25.8]	2.5–7.9	36 (46)	1.13	[1.04; 1.28]	<b>0.019</b>
Potassium (mmol/L)	4.6 [3.9; 5.7]	4.2 [3.8; 4.8]	5.4 [4.1; 6.6]	3.6–5.1	30 (38)	1.97	[1.21; 3.63]	<b>0.014</b>
Creatinine (µmol/L)	123 [72; 219]	87 [58; 123]	168 [91; 326]	53–106	36 (46)	1.004	[1.001; 1.01]	0.07
Creatinine > 177 µmol/L	15 (35)	2 (12)	13 (50)		36 (46)	7.5	[1.67; 53.9]	<b>0.018</b>
Sodium (mmol/L)	126 [123; 132]	125.0 [123; 129]	127 [123; 133]	128–145	28 (35)	0.99	[0.96; 1.05]	0.97
Calcium (mmol/L)	1.89 [1.74; 2.03]	1.95 [1.89; 1.99]	1.84 [1.72; 2.03]	2–2.58	26 (33)	0.19	[0.012; 1.75]	0.18
<b>Blood cell counts</b>								
White Blood Cells (10 <sup>3</sup> U)	14.3 [9.5; 23.3]	11.1 [7.8; 19.2]	16.4 [12.5; 23.3]	4.3–5.7	56 (71)	1.00	[0.99; 1.00]	0.88
Lymphocytes (%)	39 [26; 52]	35 [27; 50]	46 [27; 50]	20–40	56 (71)	1.01	[0.96; 1.07]	0.76
Monocytes (%)	1 [0; 3]	1 [0.5; 2.5]	1 [0; 3]	2–10	57 (72)	0.86	[0.56; 1.14]	0.33
<b>Liver function</b>								
Aspartate aminotransferase (U/L)	267 [70; 1075]	200 [46; 791]	670 [206; 1292]	11–38	60 (76)	1.001	[0.99; 1.002]	0.29
Aspartate aminotransferase > 120 U/L	12 (63)	6 (55)	6 (75)		60 (76)	2.5	[0.37; 22.7]	0.37
Alanine aminotransferase (U/L)	712 [280; 1250]	460 [101; 780]	1210 [511; 1519]	10–47	31 (39)	1.002	[1.001; 1.003]	<b>0.003</b>
Alkaline phosphatase (U/L)	296 [125; 554]	183 [96; 318]	483 [161; 774]	42–141	36 (46)	1.002	[3.10 <sup>-5</sup> ; 1.004]	0.09
Albumin (g/L)	24 [21; 28]	26 [23; 29]	24 [20; 27]	33–55	26 (33)	0.92	[0.82; 1.03]	0.16
Total protein (g/L)	66 [58; 71]	70 [59; 73]	65 [58; 69]	64–81	26 (33)	0.96	[0.90; 1.02]	0.21
<b>Other</b>								
Total bilirubin (µmol/L)	14 [10; 30]	11 [10; 14]	20 [11.0; 33]	3–27	27 (34)	1.09	[1.03; 1.18]	<b>0.013</b>
<b>Clinical symptoms</b>								
Facial/Neck swelling	43(61)	17 (50)	26 (70)		8 (10)	2.36	[0.90; 6.41]	0.084
Severe CNS manifestations	35 (53)	14 (42)	21 (64)		13 (16)	2.37	[0.89; 6.54]	0.087
Bleeding	31 (43)	14 (42)	21 (64)		13 (16)	2.37	[0.90; 6.22]	0.085
Diffuse abdominal pain / tenderness	45 (74)	20 (65)	25 (83)		18 (23)	2.75	[0.85; 9.95]	0.10
Coughing	57 (79)	25 (71)	32 (86)		7 (9)	2.56	[0.80; 9.12]	0.12
Persistent hypotension	27 (44)	12 (38)	15 (52)		18 (23)	1.79	[0.65; 5.05]	0.27
Retrosternal pain	45 (71)	21 (66)	24 (77)		16 (20)	1.80	[0.60; 5.68]	0.30
Headache	63 (94)	32 (97)	31 (91)		12 (15)	0.32	[0.02; 2.68]	0.34
Sore throat	55 (77)	24 (73)	31 (82)		8 (10)	1.66	[0.54; 5.27]	0.38
Nausea	45 (66)	21 (64)	24 (69)		11 (14)	1.25	[0.45; 3.45]	0.67
Diarrhea generalized	36 (51)	17 (50)	19 (53)		9 (11)	1.12	[0.44; 2.87]	0.82
Myalgia or arthralgia	71 (97)	34 (97)	37 (97)		6 (8)	1.09	[0.04; 28.24]	0.95

Quantitative data were presented in Median [Q1; Q3] and qualitative data with n (%). Frequencies of missing values were described with n (%). OR: odds-ratio with associated *p*-value of Wald test. In bold significant values with *p* < 0.05. Bleeding was defined as the presentation of vomiting blood, bleeding gums, bleeding nose, bloody stools or bleeding at injection sites, coughing blood or vaginal bleeding. Severe CNS manifestations was defined as the presence of disorientation, tremors or seizures. Generalized myalgia or arthralgia was observed if patients suffered from muscle pain, joint pain or general malaise. Persistent hypotension was identified by a systolic blood pressure strictly inferior to 90 mm Hg or a diastolic blood pressure strictly inferior to 60 mm Hg.

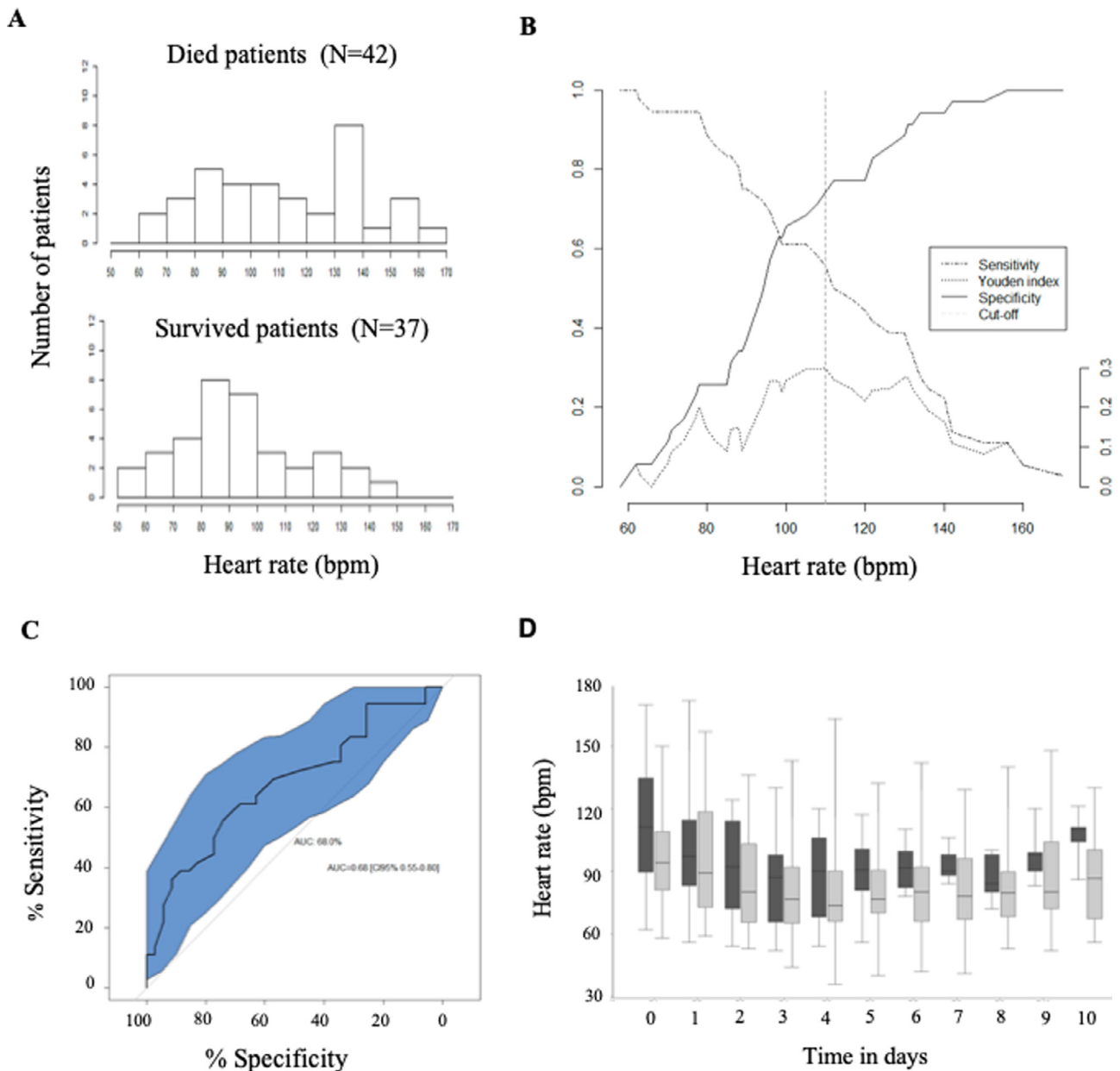


**Fig. 1.** The heart rate at admission is associated with a higher risk of mortality for the 79 LASV-infected patients.

(A) Frequency of heart rate in died and survived LASV-infected patients. (B) Youden index and its associated cutoff point for the heart rate in the 79 LASV-infected patients. Youden's maximum is 0.30, which is an optimal threshold estimated at 110 bpm. (C) ROC curve of the patients according to the outcome (died or survived), adjusted for the heart rate. (D) Longitudinal description of the heart rate during the first ten days following the admission for the patients according to the outcome. Died patients are represented by black bars and survival patients by gray bars.

### Acknowledgement

We thank Dr D. Grant for very helpful discussion, and also B. Bayon and V. Koroma from the Kenema Government Hospital (Kenema, Sierra Leone) for their contribution

### References

- McCormick J.B., Webb P.A., Krebs J.W., Johnson K.M., Smith E.S. A prospective study of the epidemiology and ecology of Lassa fever. *J Infect Dis* 1987;**155**(3):437–44.
- Hallam H.J., Hallam S., Rodriguez S.E., Barrett A.D.T., Beasley D.W.C., Chua A., et al. Baseline mapping of Lassa fever virology, epidemiology and vaccine research and development. *NPJ Vaccines* 2018;**3**:11. <https://doi.org/10.1038/s41541-018-0049-5>.
- Prescott J.B., Marzi A., Safronetz D., Robertson S.J., Feldmann H., Best S.M. Immunobiology of Ebola and Lassa virus infections. *Nat Rev Immunol* 2017;**17**(3):195–207. <https://doi.org/10.1038/nri.2016.138>.
- Okokhere P., Colubri A., Azubike C., Iruolagbe C., Osazuwa O., Tabrizi S., et al. Clinical and laboratory predictors of Lassa fever outcome in a dedicated treatment facility in Nigeria: a retrospective, observational cohort study. *Lancet Infect Dis* 2018;**18**(6):684–95. [https://doi.org/10.1016/S1473-3099\(18\)30121-X](https://doi.org/10.1016/S1473-3099(18)30121-X).
- Trombley A.R., Wachter L., Garrison J., Buckley-Beason V.A., Jahrling J., Hensley L.E., et al. Comprehensive panel of real-time Taqman polymerase chain reaction assays for detection and absolute quantification of filoviruses, arenaviruses, and New World hantaviruses. *Am J Trop Med Hyg* 2010;**82**(5):954–60. <https://doi.org/10.4269/ajtmh.2010.09-0636>.
- Shaffer J.G., Grant D.S., Schieffelin J.S., Boisen M.L., Goba A., Hartnett J.N., et al. Lassa fever in post-conflict Sierra Leone. *PLoS Negl Trop Dis* 2014;**8**(3):e2748. <https://doi.org/10.1371/journal.pntd.0002748>.
- Fluss R., Faraggi D., Reiser B. Estimation of the Youden index and its associated cutoff point. *Biom J* 2005;**147**(4):458–72. <https://doi.org/10.1002/bimj.200410135>.
- Bah E.I., Lamah M.C., Fletcher T., Jacob S.T., Brett-Major D.M., Sall A.A., et al.

Available online 3 February 2020

- Clinical presentation of patients with Ebola virus disease in Conakry, Guinea. *N Engl J Med* 2015;**372**(1):40–7. <https://doi.org/10.1056/NEJMoa1411249>.
9. Ofiaz M.B., Bolat F., Kaya A., Guven A.S., Kucukdurmaz Z., Karapinar H., et al. Resting heart rate in children with Crimean-Congo hemorrhagic fever: a tool to identify patients at risk? *Vector Borne Zoonotic Dis* 2014;**14**(1):59–65. <https://doi.org/10.1089/vbz.2013.1384>.
10. Andersen K.G., Shapiro B.J., Matranga C.B., Sealton R., Lin A.E., Moses L.M., et al. Clinical sequencing uncovers origins and evolution of Lassa virus. *Cell* 2015;**162**(4):738–50. <https://doi.org/10.1016/j.cell.2015.07.020>.

<https://doi.org/10.1016/j.jinf.2020.01.021>

© 2020 The British Infection Association. Published by Elsevier Ltd. All rights reserved.

Nadia Wauquier<sup>1</sup>

Sorbonne Université, Inserm U1135, CNRS ERL 8255, Centre d'Immunologie et des Maladies Infectieuses (CIMI-Paris), Paris, France  
Metabiota Inc., Silver Spring and San Francisco, United States

Camille Couffignal<sup>1</sup>, Pauline Manchon

AP-HP, Hôpital Bichat, IAME, Inserm UMR 1137, Université Paris Diderot, Paris, France

Elisabeth Smith

Metabiota Inc., Freetown, Sierra Leone

Victor Lungay

Ministry of Health and Sanitation, Sierra Leone

Moinya Coomber

Sierra Leone Ministry of Health and Sanitation, Sierra Leone

Lauren Weisenfluh

Department of Epidemiology, Columbia University, New York, NY, United States

James Bangura

Kenema Government Hospital, Kenema, Sierra Leone

Sheik Humarr Khan

Ministry of Health and Sanitation, Sierra Leone

Amara Jambai

Kenema Government Hospital, Kenema, Sierra Leone

Aiah Gbakima

Ministry of Health and Sanitation, Sierra Leone

Nadezda Yun, Slobodan Paessler

Galveston National Laboratory, University of Texas Medical Branch, Galveston, TX, United States

Randal Schoepp

U.S. Army Medical Research Institute of Infectious Diseases, Fort Detrick, MD, United States

Stephen S. Morse

Department of Epidemiology, Mailman School of Public Health, Columbia University, New York, NY, United States

Jean-Paul Gonzalez, Joseph Fair

Metabiota Inc., Silver Spring and San Francisco, United States

France Mentré

AP-HP, Hôpital Bichat, IAME, Inserm UMR 1137, Université Paris Diderot, Paris, France

Vincent Vieillard\*

Sorbonne Université, Inserm U1135, CNRS ERL 8255, Centre d'Immunologie et des Maladies Infectieuses (CIMI-Paris), Paris, France

\*Corresponding author at: Center of Immunology and Infectious Diseases, Pitié-Salpêtrière hospital, 83 Boulevard de l'hôpital, 75013 Paris, France.

E-mail address: [vincent.vieillard@sorbonne-universite.fr](mailto:vincent.vieillard@sorbonne-universite.fr) (V. Vieillard)

## Codon usage bias of H3N8 equine influenza virus – An evolutionary perspective



Dear Editor,

Recently, several reports in the *Journal of Infection* have demonstrated the codon usage bias of influenza virus.<sup>1–3</sup> Equine influenza (EI) is a severe and highly contagious disease in horses. Equine influenza virus (EIV) is the antigen that causes this important horse disease.<sup>4</sup> The prevalent subtype of the virus is H3N8.<sup>5</sup> To our knowledge, an evolutionary analysis of codon usage bias of H3N8 EIV has not been investigated. HA and NA are its main surface proteins, responsible for binding the virus to the cell and releasing progeny virus, respectively. These two important genes of H3N8 EIV were used in this study to perform an evolutionary analysis of codon usage bias.

The complete coding sequences for the HA and NA genes of H3N8 subtype EIV were downloaded from the online influenza sequence database (<http://www.ncbi.nlm.nih.gov/genomes/FLU/FLU.html>). The sequences containing non-translational codons were not included in our study. The effective number of codons (ENC) was introduced using the formula:  $ENC = 2 + S + \{29 / [S^2 + (1 - S)^2]\}$ , where  $S$  are the GC3s in the gene. The ENC value was completely influenced by the GC3s<sup>6,7</sup>. The codon adaptation index (CAI) was employed to study the adaptation of EIV to the host cell. The synonymous codon usage patterns of the viral host of *Equus caballus* (horse) were obtained from the online database (<http://www.kazusa.or.jp/codon/>). CAI values were calculated using the online tool CALcal (<http://genomes.urv.es/CALcal>)<sup>8,9</sup>. Neutral evolution analysis can explain whether natural selection pressure or mutation bias plays a more important role in shaping codon usage patterns<sup>10</sup>. In our analysis,  $P12$  (the average GC content of the GC1s and GC2s) was plotted against  $P3$  (the GC3s). The role of natural selection or mutation bias could then be determined by the slope of a simple regression line. All of the graphics were generated in GraphPad Prism 5.0. Correlation analysis was carried out using the statistical software SPSS 19.0. The relationships were considered to be correlation, significant correlation or extremely significant correlation if  $0.01 < p < 0.05$ ,  $0.001 < p < 0.01$ , or  $p < 0.001$ , respectively.

The average ENC values of HA and NA were 48.9 and 50.3, respectively, indicating a low codon usage bias. To perform an evolutionary analysis of codon usage patterns, the ENC and CAI values were plotted against evolutionary time (Fig. 1). The ENC values of both HA and NA were significantly correlated with time (Fig. 1(A)). The overall ENC values of HA and NA gradually decreased when EIV was under constant evolution. These rates of change were  $-0.1056 \pm 0.0043$  and  $-0.0859 \pm 0.0044$  of the ENC values per year for HA and NA, respectively. This showed that codon usage patterns in HA and NA grew increasingly biased, especially in HA. The CAI value shown in Fig. 1(B) was correlated, significantly correlated with changes in time, revealing that the CAI value was generally decreasing. However, the low rate of change of the CAI value against HA and NA was  $-0.4679 \pm 0.2758 \times 10^{-4}$  and  $-0.4828 \pm 0.2576 \times 10^{-4}$  for horse, respectively, indicating a low decreasing trend in EIV's adaption to its host.

<sup>1</sup> These authors contributed equally to this article.



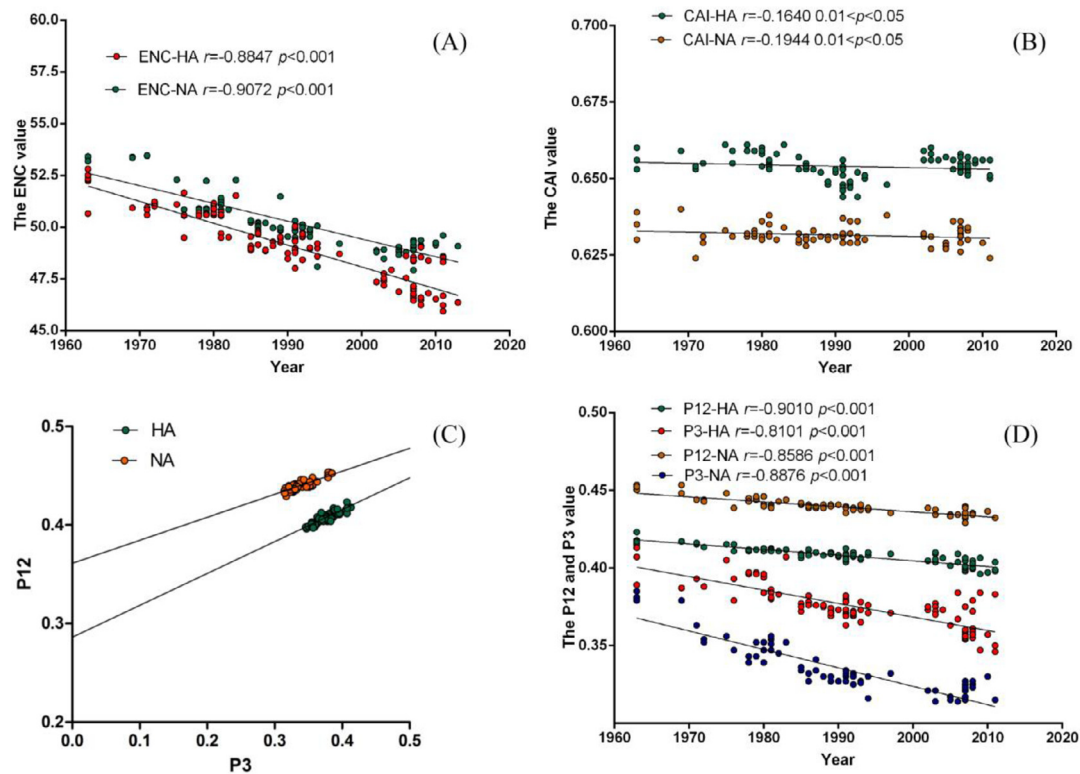


Fig. 1. The evolutionary analysis of the ENC and CAI values plotted against evolutionary time (A) for the ENC values, (B) the CAI values, and (C) (D)  $P12$  and  $P3$  values.

Neutral analysis revealed  $P12$  was extremely significantly correlated with  $P3$  in both the HA ( $r=0.8636$ ,  $p<0.001$ ) and NA ( $r=0.8324$ ,  $p<0.001$ ) genes (Fig. 1(C)). The correlation coefficients for HA and NA were  $0.3234 \pm 0.018$  and  $0.2334 \pm 0.0016$ , respectively. Thus the relative neutrality is 32.34% for HA and 23.34% for NA, and a relative constraint on  $P3$  (0% constraint) is 67.66% for HA and 76.66% for NA. This indicates that natural selection pressure predominated over mutation bias in the coding sequences of the HA and NA genes in H3N8 EIV.  $P12$  and  $P3$  values were negatively extremely significantly correlated with time (Fig. 1(D)). The correlation coefficients for  $P12$  and  $P3$  in HA were  $-3.639 \pm 0.170 \times 10^{-4}$  and  $-8.680 \pm 0.607 \times 10^{-4}$ , respectively. The correlation coefficients for  $P12$  and  $P3$  of in NA were  $-3.219 \pm 0.203 \times 10^{-4}$  and  $-11.87 \pm 0.65 \times 10^{-4}$ , respectively. The GC3s always decreased with a higher rate than the GC12s, indicating that natural selection pressure played an increasingly critical role in the codon usage pattern of both the HA and NA genes when H3N8 EIV evolved.

In summary, our study indicated the codon usage bias of H3N8 EIV became increasingly biased, and natural selection played an increasingly important role in shaping the codon usage pattern in the evolutionary procession. These conclusions provide important insight into the codon usage bias of H3N8 EIV as well as a better understanding of its evolutionary pattern.

#### Declaration of Competing Interests

The authors declare not conflict of interest.

#### Acknowledgments

This work was supported by the Guangdong Provincial Natural Science Foundation [grant number 2017A030310367].

#### References

- Luo W., Tian L., Huang C.Q., Li J.Y., Shen X.J., Robert W.M., et al. The codon usage bias of avian influenza A viruses. *J Infect* 2019;**79**:175–7.
- Guo F.C., Shen X.J., Irwin D.M., Shen Y.Y. Avian influenza A viruses H5Nx (N1, N2, N6 and N8) show different adaptations of their codon usage patterns to their hosts. *J Infect* 2019;**79**:181–3.
- Luo W., Li Y.L., Yu S., Shen X.J., Tian L., David M.L., et al. Better fit of codon usage of the polymerase and nucleoprotein genes to the chicken host for H7N9 than H9N2 AIVs. *J Infect* 2019;**79**:174–5.
- Sack A., Cullinane A., Daramragchaa U., Chuluunbaatar M., Gonchigoo B., Gray G.C. Equine influenza virus – a neglected, reemerging disease threat. *Emerg Infect Dis* 2019;**25**:1185–91.
- Daly J.M., MacRae S., Newton J.R., Wattring E., Elton D.M. Equine influenza: a review of an unpredictable virus. *Vet J* 2011;**189**:7–14.
- Lu G., Guo W., Qi T., Ma J., Zhao S., Tian Z., et al. Genetic analysis of the PB1-F2 gene of equine influenza virus. *Virus Genes* 2013;**47**:250–8.
- Sharp P.M., Li W.H. Codon usage in regulatory genes in *Escherichia coli* does not reflect selection for 'rare' codons. *Nucleic Acids Res* 1986;**14**:7737–49.
- Puigbo P., Bravo I.G., Garcia-Valve S. CAIcal: a combined set of tools to assess codon usage adaptation. *Biol Direct* 2008;**3**:38.
- Sharp P.M., Li W.H. The codon adaptation index – a measure of directional synonymous codon usage bias, and its potential applications. *Nucleic Acids Res* 1987;**15**:1281–95.
- Zhao S., Zhang Q., Chen Z.H., Zhong J.C. The factors dictating the codon usage variation among the genes in the genome of burkholderia pseudomallei. *World J Microbiol Biotechnol* 2008;**24**:1585–92.

Jiajun Ou<sup>1</sup>

College of Veterinary Medicine, South China Agricultural University, Guangzhou 510642, Guangdong Province, People's Republic of China  
Guangdong Provincial Key Laboratory of Prevention and Control for Severe Clinical Animal Diseases, Guangzhou 510642, Guangdong Province, People's Republic of China  
Guangdong Technological Engineering Research Center for Pet, Guangzhou 510642, Guangdong Province, People's Republic of China

Ruijie Chen<sup>1</sup>

College of Veterinary Medicine, South China Agricultural University, Guangzhou 510642, Guangdong Province, People's Republic of China

Zhaoqing Institute of Biotechnology Co., Ltd, Zhaoqing 526238,  
Guangdong Province, People's Republic of China

Zhongshan Yan, Shudan Ou  
College of Veterinary Medicine, South China Agricultural University,  
Guangzhou 510642, Guangdong Province, People's Republic of China  
Guangdong Provincial Key Laboratory of Prevention and Control for  
Severe Clinical Animal Diseases, Guangzhou 510642, Guangdong  
Province, People's Republic of China  
Guangdong Technological Engineering Research Center for Pet,  
Guangzhou 510642, Guangdong Province, People's Republic of China

Nan Dong  
Zhaoqing Institute of Biotechnology Co., Ltd, Zhaoqing 526238,  
Guangdong Province, People's Republic of China

Gang Lu\*, Shoujun Li\*  
College of Veterinary Medicine, South China Agricultural University,  
Guangzhou 510642, Guangdong Province, People's Republic of China  
Guangdong Provincial Key Laboratory of Prevention and Control for  
Severe Clinical Animal Diseases, Guangzhou 510642, Guangdong  
Province, People's Republic of China  
Guangdong Technological Engineering Research Center for Pet,  
Guangzhou 510642, Guangdong Province, People's Republic of China

\*Corresponding authors.

E-mail addresses: [lg@scau.edu.cn](mailto:lg@scau.edu.cn) (G. Lu), [shoujunli@scau.edu.cn](mailto:shoujunli@scau.edu.cn) (S. Li)

<sup>1</sup> Contributed equally to this study.  
Accepted 8 January 2020  
Available online 17 January 2020

<https://doi.org/10.1016/j.jinf.2020.01.004>

© 2020 The British Infection Association. Published by Elsevier Ltd. All rights reserved.

## Identification of the hyper-variable genomic hotspot for the novel coronavirus SARS-CoV-2



### Dear Editor,

A recent study in this journal studied the genomes of the novel SARS-like coronavirus (SARS-CoV-2) in China and suggested that the SARS-CoV-2 had undergone genetic recombination with SARS-related CoV<sup>1</sup>. By February 14, 2020, a total of 66,576 confirmed cases of COVID-19, people infected with SARS-CoV-2, were reported in China, leading to 1524 deaths, per the Chinese CDC (<http://2019ncov.chinacdc.cn/2019-nCoV/>). Several full genomic sequences of this virus have been released for the study of its evolutionary origin and molecular characteristics<sup>2–4</sup>. Here, we analyzed the potential mutations that may have evolved after the virus became epidemic among humans and also the mutations resulting in the human adaptation.

The sequences of BetaCoV were downloaded on February 3, 2020 from the GISAID platform<sup>5</sup>. A total of 58 accessions were available, among which BetaCoV/bat/Yunnan/RaTG13/2013 is a known close relative of SARS-CoV-2. Four accessions, namely, BetaCov/Italy/INM1/2020, BetaCov/Italy/INM2/2020, BetaCov/Kanagawa/1/2020, and BetaCoV/USA/IL1/2020, were excluded because of the short-truncated sequences or multiple ambiguous nucleotides. A total of 54 accessions (Supplementary Table 1) isolated from humans were utilized in the following analysis. The sequences NC\_004718.3 of SARS coronavirus<sup>6</sup> genes were utilized

to define the protein products of SARS-CoV-2. The protein sequences of ORF1ab, S, E, M, and N genes were translated, and all of the loci without experimental evidences were excluded. First, the protein sequences of SARS-CoV-2 were compared with RaTG13, human SARS (NC\_004718.3), bat SARS (DQ022305.2), and human MERS (NC\_019843.3) by calculating the similarity in a given sliding window (Fig. 1A). The sliding window was set to 500 for ORF1ab and S, and to 50 for proteins E, M, and N considering their short length. SARS-CoV-2 were highly similar to RaTG13 isolated from bats, showing 96% identity based on the whole-nucleotide sequences and 83% based on the protein sequences, suggesting a bat zoonotic origin of SARS-CoV-2. ORF1a, and the head of S seemed to have diverged from other beta coronaviruses.

The molecular phylogenetic tree (Fig. 1B) was built by using the maximum likelihood method based on the JTT matrix-based model<sup>7</sup>. It hinted that the protein sequences of SARS-CoV-2 had over 99% similarity. Twenty-eight viruses had shared the same protein sequences, and could be the original strain circulated in the humans. The other viruses had only a few mutations from it. This indicates that the virus could have evolved for only a very short time after gaining the efficient human to human transmissibility, as expected. Next, we analyzed the mutations that occurred after infecting humans (Fig. 1C) in order to identify mutations associated with more severe infection. Here, two accessions (BetaCoV/Shenzhen/SZTH-001/2020 and BetaCoV/Shenzhen/SZTH-004/2020) from Shenzhen, which had 5 and 16 mutations, respectively, were excluded, considering the possible experimental issues. All of the mutations only occurred once, so it is possible that all of these mutations occur naturally and are associated with viral survival and infection. Several mutations were clustered in peptides nsp3 and nsp4 of ORF1ab and in the header of S. These results suggested that there had probably been no hyper-variable genomic hotspot in the SARS-CoV-2 population until now.

We compared these results with those of the work of Ceraolo and Giorgi<sup>8</sup>, who reported at least two hyper-variable genomic hotspots based on the Shannon entropy of nucleotide sequences. They utilized all of the sequences, while we merged all of the fully identical sequences into one during our Shannon entropy calculation. As shown in Fig. 1B, 28 sequences were merged into one in present study because they had been collected in such a short time, so collection time and location could not have produced any large bias. If those identical sequences were calculated individually, any mutations on these 28 sequences would have sharply increased Shannon entropy. The protein sequences were used to exclude any unimportant silent mutations. Finally, the sequences of earliest SARS-CoV-2 were compared with RaTG13 from bats (Fig. 1D). Fisher's exact test with post hoc test suggested that nsp1, nsp3, and nsp15 of ORF1ab and gene S had significantly more mutations than other genes, which might facilitate human adaptation and infection.

S gene encodes spike glycoprotein, which binds host ACE2 receptors and is required for initiation of the infection<sup>9</sup>. They reported that a 193-amino acid fragment was able to bind ACE2 more efficiently than its unmutated counterpart. This region in which spike glycoprotein binds to ACE2 had 21 mutations not found in RaTG13, suggesting their role in the adaptation to human hosts. Peptide nsp1 facilitated viral gene expression and evasion from the host immune response<sup>10</sup>. Peptide nsp3, named papain-like proteinase, was found to be associated with the cleavages, viral replication, and antagonization of innate immune. These two peptides are probably associated with the latent period after infection in humans. Peptide nsp15 acted as uridylylate-specific endoribonuclease. These results collectively suggest that peptides nsp1, nsp3, and nsp15 might have unclear but critical roles in this outbreak of SARS-CoV-2.

To summarize, this study confirmed the relationship of SARS-CoV-2 with other beta coronaviruses on the amino acid level.

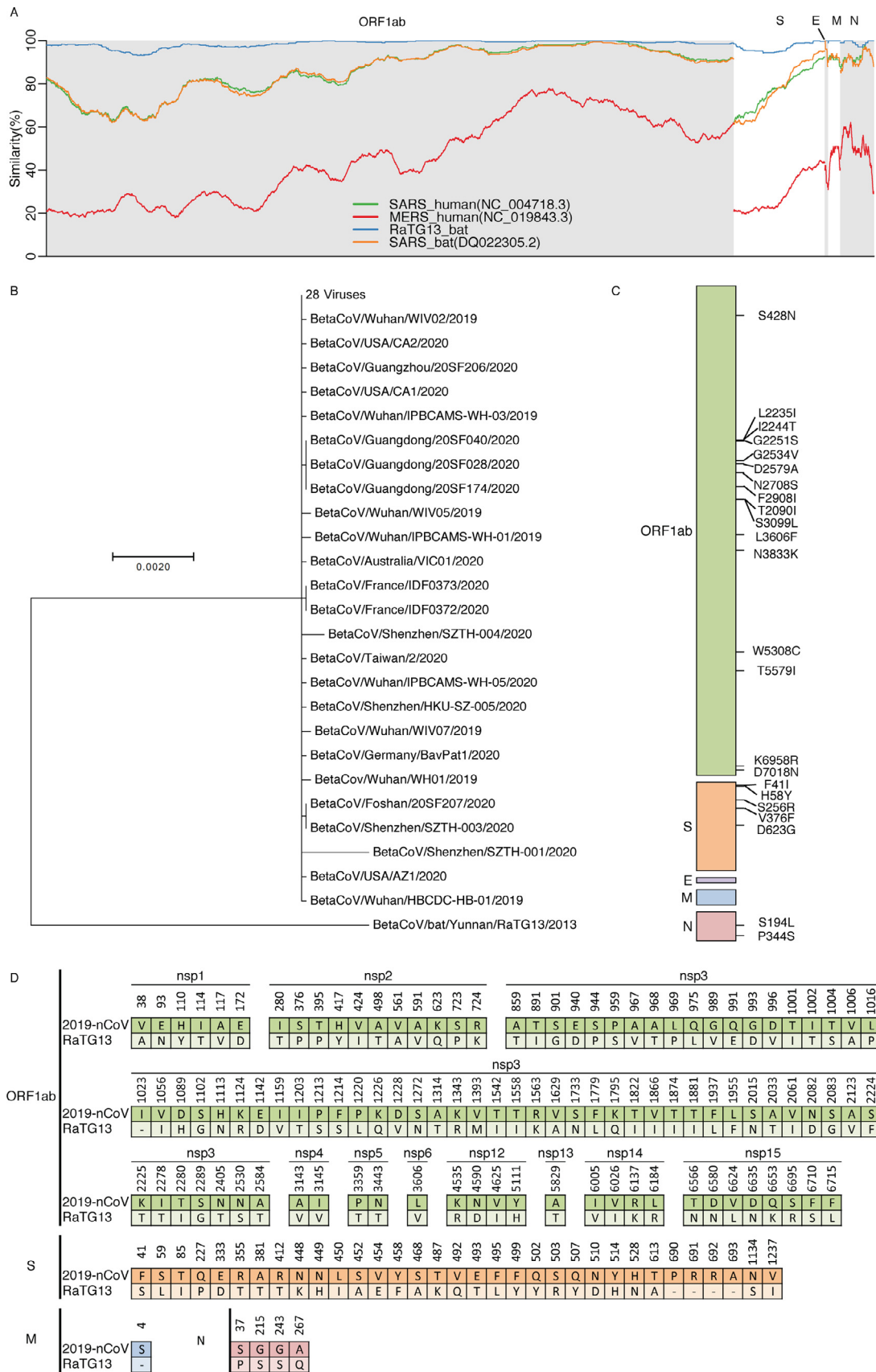


**Fig. 1.** (A) The similarity between SARS-CoV-2 and other beta coronaviruses using the sliding window showed that SARS-CoV-2 was similar to bat virus RaTG13. (B) The molecular phylogenetic tree based on protein sequences established the high similarity among SARS-CoV-2 and its near relatives. (C) The mutations that developed after it came to circulate among humans did not include any mutation with high occurrence. (D) The graphs show all of the differences between SARS-CoV-2 and its close relative strains isolated from bats.

The hyper-variable genomic hotspot has been established in the SARS-CoV-2 population at the nucleotide but not the amino acid level, suggesting that there have been no beneficial mutations. The mutations in nsp1, nsp3, nsp15, and gene S that identified in this study would be associated with the SARS-CoV-2 epidemic and was worthy of further study.

### Declaration of Competing Interest

None.

### Funding

This study was supported by Key Laboratory for Preventive Research of Emerging Animal Diseases in Foshan University (KLPREAD201801-06), (KLPREAD201801-10), Youth Innovative Talents Project of Guangdong Province (2018KQNCX280), and National Key Research and Development Project (grant No.2017YFD0500800).

### Acknowledgement

We thank the researchers who deposited the SARS-CoV-2 sequences in the GISAID. We thank LetPub for its linguistic assistance during the preparation of this manuscript.

### Supplementary materials

Supplementary material associated with this article can be found, in the online version, at doi:10.1016/j.jinf.2020.02.027.

### References

- Zhang J., Ma K., Li H., Liao M., Qi W.. The continuous evolution and dissemination of 2019 novel human coronavirus. *J. Infect.* 2020.
- Wu A., Peng Y., Huang B., Ding X., Wang X., Niu P., et al. Genome composition and divergence of the novel coronavirus (2019-nCoV) originating in China. *Cell Host Microbe* 2020.
- Wu F., Zhao S., Yu B., Chen Y.M., Wang W., Song Z.G., et al. A new coronavirus associated with human respiratory disease in China. *Nature* 2020.
- Zhou P., Yang X.L., Wang X.G., Hu B., Zhang L., Zhang W., et al. A pneumonia outbreak associated with a new coronavirus of probable bat origin. *Nature* 2020.
- Shu Y., McCauley J.. GISAID: global initiative on sharing all influenza data - from vision to reality. *Euro. Surveill.* 2017;22(13).
- Marra M.A.. The genome sequence of the SARS-associated coronavirus. *Science* 2003;300(5624):1399–404.
- Jones D.T., Taylor W.R., Thornton J.M.. The rapid generation of mutation data matrices from protein sequences. *Comput. Appl. Biosci.* 1992;8(3):275–82.
- Ceraolo C., Giorgi F.M.. Genomic variance of the 2019-nCoV coronavirus. *J. Med. Virol.* 2020.
- Wong S.K., Li W., Moore M.J., Choe H., Farzan M.. A 193-amino acid fragment of the SARS coronavirus S protein efficiently binds angiotensin-converting enzyme 2. *J Biol Chem* 2004;279(5):3197–201.
- Lokugamage K.G., Narayanan K., Huang C., Makino S.. Severe acute respiratory syndrome coronavirus protein nsp1 is a novel eukaryotic translation inhibitor that represses multiple steps of translation initiation. *J. Virol.* 2012;86(24):13598–608.

Feng Wen\*<sup>1</sup>

College of Life Science and Engineering, Foshan University, Foshan, 528231 Guangdong, China

Hai Yu<sup>1</sup>

Shanghai Veterinary Research Institute, Chinese Academy of Agricultural Sciences, Shanghai 200241, China  
Jiangsu Co-innovation Center for Prevention and Control of Important Animal Infectious Diseases and Zoonoses, Yangzhou 225009, China

Jinyue Guo

College of Life Science and Engineering, Foshan University, Foshan, 528231 Guangdong, China

Yong Li

College of Animal Science and Technology, Jiangxi Agricultural University, Nanchang 330045 Jiangxi, China

Kaijian Luo

College of Veterinary Medicine, South China Agricultural University, Guangzhou 510642 Guangdong, China

Shujian Huang\*

College of Life Science and Engineering, Foshan University, Foshan, 528231 Guangdong, China

\*Corresponding authors.

E-mail addresses: wenfengjlu@163.com (F. Wen), 617955368@qq.com (S. Huang)

<sup>1</sup> These authors contribute equally to this work.

Accepted 29 February 2020

Available online 5 March 2020

<https://doi.org/10.1016/j.jinf.2020.02.027>

© 2020 The British Infection Association. Published by Elsevier Ltd. All rights reserved.

### Insights into the cross-species evolution of 2019 novel coronavirus



Dear Editor,

Recent study reported in this journal that the threats of continuous evolution and dissemination of 2019 novel coronaviruses.<sup>1</sup> Since its emergence in December 2019, a “seventh” member of the family of human coronavirus named “SARS-CoV-2” was responsible for an outbreak of coronavirus disease (COVID-19) in Wuhan, China.<sup>2</sup> As of March 7, 2020, China had reported more than 80,815 confirmed cases of SARS-CoV-2, with 3,073 fatalities and counting (<http://www.nhc.gov.cn>). Strikingly, SARS-CoV-2 had been transmitted rapidly in more than 90 countries to date (<https://www.who.int>), including Asia, Europe, North America, South America, Africa, and Oceania, posing serious concerns about its pandemic potential. Despite of droplet and contact transmissions of SARS-CoV-2, recent studies demonstrated that SARS-CoV-2 might be transmitted via aerosol and fecal–oral routes<sup>3</sup> (Fig. 1), which needs to be paid attention in particular.

The close phylogenetic relationship to bat-origin coronaviruses provided evidence for a bat origin of SARS-CoV-2.<sup>4</sup> Bats provided a rich “gene pool” for interspecies exchange of genetic fragments of coronaviruses, which were established as mixing vessels of different coronaviruses.<sup>5</sup> Although humans and bats live in different environments, some wildlife species were susceptible to the novel coronaviruses in nature, highlighting that the need of tracing its origin of SARS-CoV-2 in wild animals. Previously, researchers had demonstrated that coronaviruses had been detected in pangolins.<sup>6</sup> Here, we explored the phylogenetic relationship of the human SARS-CoV-2 together with pangolin- and bat-origin coronaviruses. The similarity analysis of SARS-CoV-2 and the animal-origin coronaviruses demonstrated that recombination events were likely to occur in bat- and pangolin-origin coronaviruses (Supplementary Figure S1). A Blast search of the complete genome sequences of SARS-CoV-2 suggested that the closely related coronaviruses were the BetaCoV/bat/Yunnan/RaTG13/2013 (bat/RaTG13) and BetaCoV/Pangolin/Guangdong/1/2020 (Pangolin/1), with ~96% and ~90.5% overall genome sequences identity, respectively. In the 1ab,

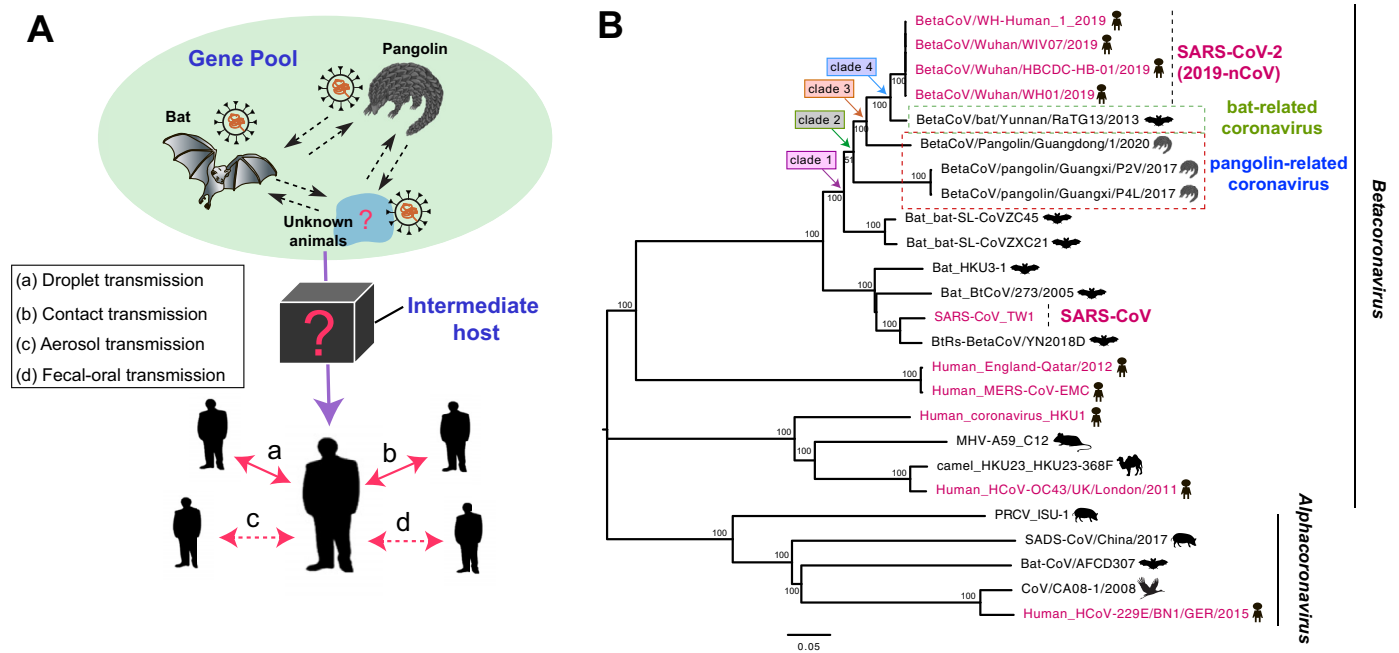


**Fig. 1.** Phylogenetic overview and putative model of transmission of SARS-CoV-2. (A) Potential routes of cross-species transmission of SARS-CoV-2. The dashed line indicates potential transmission routes. Abbreviation of SARS-CoV-2 indicates 2019 novel coronavirus. (B) The phylogenetic relationship among SARS-CoV-2 and other coronaviruses in bats, birds, mice, camels, swine, pangolins, and humans. Red color indicates the human-origin coronaviruses. The scale bar represents the number of nucleotide substitutions per site (subs/site).

S, E, M, and N genes, the bat/RaTG13 coronavirus exhibited 96.2%, 97.3%, 100%, 99.6%, and 99.0% amino acid identical to that of SARS-CoV-2, respectively, while the pangolin/1 coronavirus showed the 96.3%, 92.4%, 100%, 98.7%, and 97.9% amino acid identical to that of SARS-CoV-2, respectively (Fig. 2). However, it was notably that 1b gene sequence identity of pangolin/1 coronavirus was greater than bat-origin RaTG13 coronavirus, with the highest being 99.3%.

The spike (S) protein mediates receptor binding and membrane fusion.<sup>7</sup> The amino acids of the spike 2 protein of pangolin-origin coronaviruses and SARS-CoV-2 were more conserved than that of the spike 1 protein, and only a few minor deletions of amino acids of S protein were found in pangolin-origin coronavirus compared with the SARS-CoV-2 (Supplementary Figure S4). Interestingly, the receptor-binding domain (RBD) of SARS-CoV-2 was more similar to that of the bat/RaTG13 strain and Pangolin/1 coronavirus. Although the S amino acid identities of pangolin-origin coronavirus exhibited lower amino acid identities with bat/RaTG13, it was noteworthy that six amino acids associated with the receptor binding preference of human receptor angiotensin converting enzyme II—464L, 495F, 502Q, 503S, 510N, and 514Y (SARS-CoV-2 numbering)—in the pangolin/1 coronavirus were the same as that of SARS-CoV-2 (Fig. 2), but were distinct from that of the bat-origin coronaviruses. Besides, the PRRA-motif insertion was occurred in the S1/S2 junction of SARS-CoV-2; however, the PRRA-motif insertion in the pangolin- and bat-origin coronaviruses was missing (Supplementary Figure S4), suggesting that the convergent cross-species evolution of SARS-CoV-2-related coronaviruses.

The phylogenetic tree of full-genome of SARS-CoV-2 related coronaviruses could be classified into four clades, including clade 1, clade 2, clade 3, and clade 4 (Fig. 1). The two bat-origin SARS-like strains (bat-SL-CoVZC45 and bat-SL-CoVZXC21) formed clade 1, and pangolin-derived Pangolin/1, BetaCoV/Pangolin/Guangxi/P2V/2017 (Pangolin/P2V), and BetaCoV/Pangolin/Guangxi/P4L/2020 (Pangolin/P4L) coronaviruses formed newly independent clade 2 and clade 3, which were notable for the long branch separating the bat/RaTG13 strain and

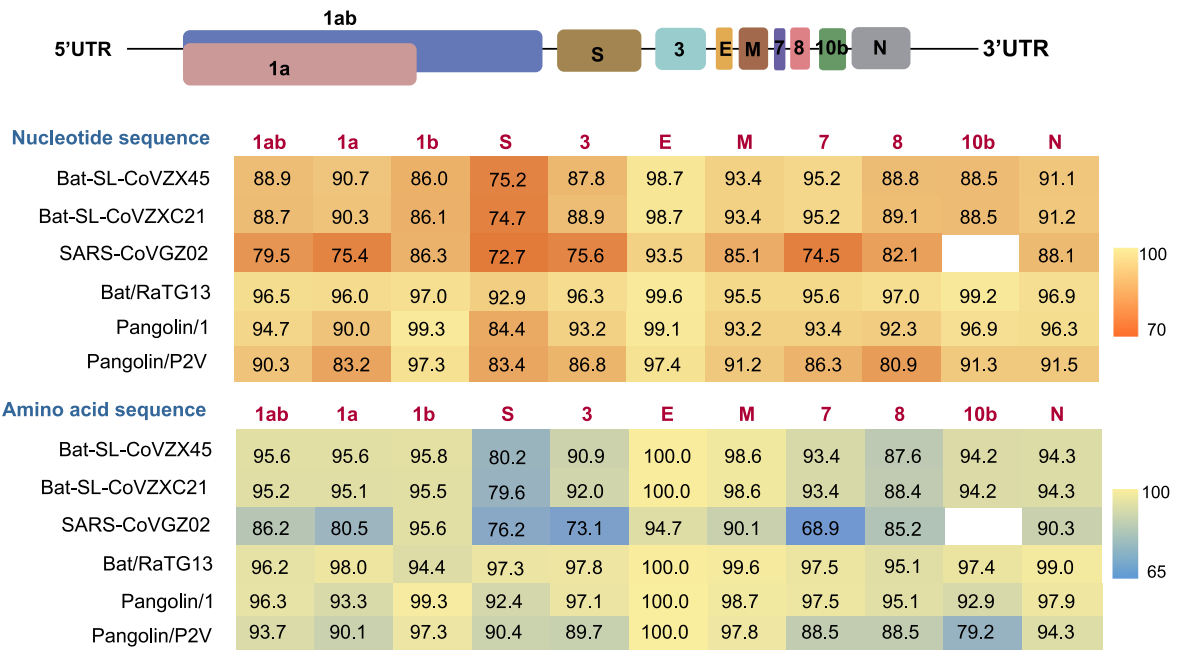
SARS-CoV-2 (Fig. 1). Of note, we found that the full genome and RNA-dependent RNA polymerase genome of Pangolin/1 coronavirus were genetically closely related to the bat/RaTG13 and SARS-CoV-2 strains (Fig. 1 and Supplementary Figure S3). However, in the phylogenetic tree of S gene, the Pangolin/P2V and Pangolin/P4L coronaviruses were more closely related to that of the bat/RaTG13 and SARS-CoV-2 strains (Supplementary Figure S2), indicative of the continuous evolution and genetic recombination of pangolin- and bat-derived coronaviruses. There was clearly a genetic gap between SARS-CoV-2 and the nearest bat- and pangolin-origin coronaviruses, and the phylogenetic relationship of pangolin-origin coronaviruses were far from that of bat/RaTG13 (Fig. 1). Given the use of pangolins use in traditional medicine and for food, what kind of role do the pangolins play in the cross-species evolution and transmission of the novel coronavirus? Further details needed to be sought in the future.

Frequent human-animal interface had been recognized the major cause for viral cross-species transmission. It is speculated that the coronaviruses circulating in pangolin, bat, and other animal species are likely perceived to be a “gene pool” for the generation of new recombinants (Fig. 1). During the long-time of co-existence of coronaviruses and their hosts, different viruses recombine with each other in multiple animal hosts to generate new recombinants, with some of them adapting to the new hosts such as humans. However, what animal species are the intermediate hosts in the transmission cascade of SARS-CoV-2. In response to such pressing question, further surveillance in natural environment of China and the rest of countries needed to be sought to understand the emergence and potential transmission of SARS-CoV-2.

#### Declaration of Competing Interest

All authors have no potential conflicts of interest to disclose.

**A**



**B**

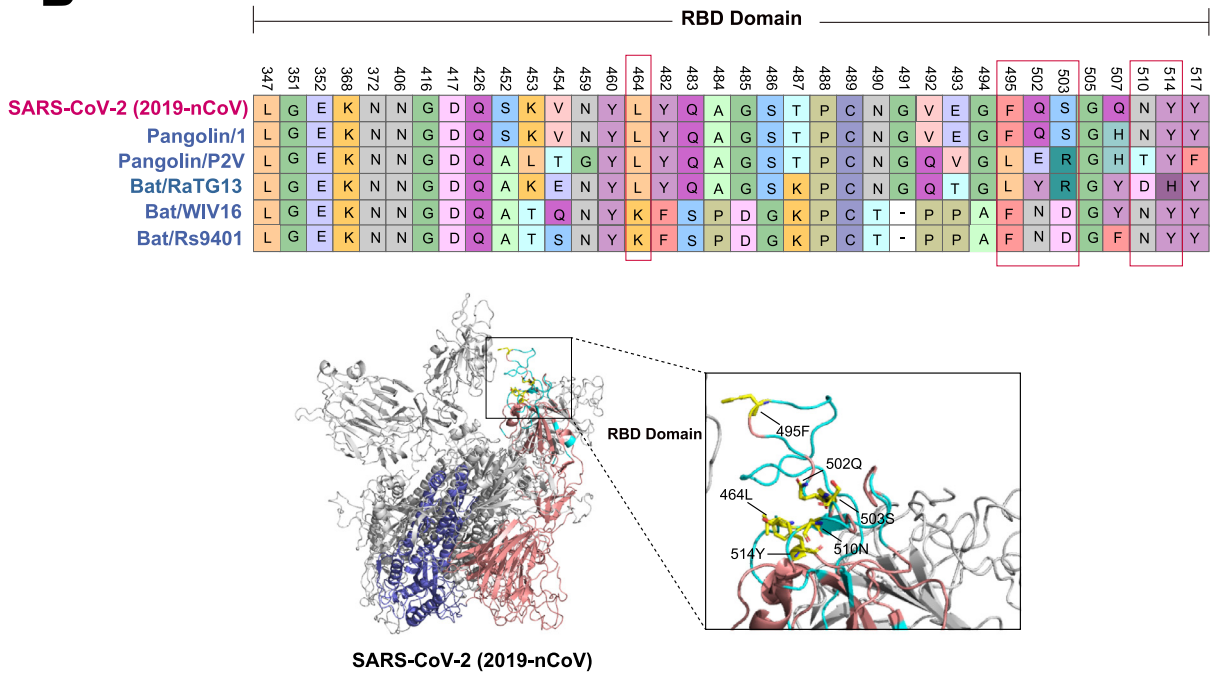


**Fig. 2.** The genomic characterization and specific amino acids variants among the receptor-binding domain of SARS-CoV-2, bat- and pangolin-origin coronaviruses. (A) The schematic diagram of the genome organization and sequence identities for SARS-CoV-2 compared with SARS-CoV GZ02 (accession number AY390556), bat SARS-like coronavirus bat-SL-CoVZXC45 (accession number MG772933), bat-SL-CoVZXC21 (accession number MG772934), BetaCoV/bat/Yunnan/RaTG13/2013 (bat/RaTG13) (accession number EPI\_ISL\_40,131), BetaCoV/Pangolin/Guangdong/1/2020 (Pangolin/1) (accession number EPI\_ISL\_410,721), and BetaCoV/Pangolin/Guangxi/P2V/2017 (Pangolin/P2V) (accession number EPI\_ISL\_410,542). (B) Amino acid substitutions of SARS-CoV-2 against bat- and pangolin-origin coronaviruses. An amino acid substitution of spike (S) protein is defined as an absolutely conserved site in the bat- and pangolin-origin coronaviruses but different from that of SARS-CoV-2. Structural analysis of S protein of SARS-CoV-2 was modelled using the Swiss-Model program (<https://swissmodel.expasy.org/>) with that of the S protein of SARS-CoV structure (Protein Data Bank ID 2DD8) as a template. The red and blue regions indicate the spike protein 1 and spike protein 2, respectively. The wathet blue region of SARS-CoV-2 indicates the receptor binding region. The correspondencing amino acids to the three-dimensional (3D) structure of the S protein of SARS-CoV-2 were mapped using MacPymol (<http://www.pymol.org/>).

## Acknowledgement

We sincerely thank the authors of the human 2019 coronavirus from GISAID EpiFlu™ Database. This work was supported by National Natural Science Foundation of China (31941014, 31830097, 31672586), the Key Research and Development Program of Guangdong Province (2019B020218004), Earmarked Fund for China Agriculture Research System (CARS-41-G16), Guangdong Province Universities and Colleges Pearl River Scholar Funded Scheme (2018, Wenbao Qi), and Young Scholars of Yangtze River Scholar Professor Program (2019, Wenbao Qi).

## Supplementary materials

Supplementary material associated with this article can be found, in the online version, at doi:10.1016/j.jinf.2020.02.025.

## References

- Zhang J., Ma K., Li H., Liao M., Qi W.. The continuous evolution and dissemination of 2019 novel human coronavirus. *J Infect* 2020. doi:10.1016/j.jinf.2020.02.001.
- Gorbalenya A.E.. Severe acute respiratory-related coronavirus—The species and its viruses, a statement of the Coronavirus Study Group. *BioRxiv* 2020. doi:10.1101/2020.02.07.937862.
- Guan W., Ni Z., Hu Y., Liang W., Ou C., He J., et al. Clinical characteristics of 2019 novel coronavirus infection in China. *MedRxiv* 2020. doi:10.1101/2020.02.06.20020974.
- Zhou P., Yang X., Wang X., Hu B., Zhang L., Zhang W., et al. A pneumonia outbreak associated with a new coronavirus of probable bat origin. *Nature* 2020. <https://doi.org/10.1038/s41586-020-2012-7>.
- Hu B., Zeng L., Yang X., Ge X., Zhang W., Li B., et al. Discovery of a rich gene pool of bat SARS-related coronaviruses provides new insights into the origin of SARS coronavirus. *Plos Pathog* 2017;13(11):e1006698.
- Liu P., Chen W., Chen J.. Viral metagenomics revealed sendai virus and coronavirus infection of Malayan Pangolins (*Manis javanica*). *Viruses* 2019;11(11) pii: E979.
- Lu G., Wang Q., Gao G.F.. Bat-to-human: spike features determining 'host jump' of coronaviruses SARS-CoV, MERS-CoV, and beyond. *Trends Microbiol* 2015;23:468–78.

Jiahao Zhang<sup>1</sup>

National and Regional Joint Engineering Laboratory for Medicament of Zoonoses Prevention and Control, South China Agricultural University, Guangzhou 510642, PR China  
Key Laboratory of Zoonoses Prevention and Control of Guangdong Province, Guangzhou 510642, PR China

Weixin Jia<sup>1</sup>

National and Regional Joint Engineering Laboratory for Medicament of Zoonoses Prevention and Control, South China Agricultural University, Guangzhou 510642, PR China  
Key Laboratory of Zoonoses, Ministry of Agriculture and Rural Affairs, Guangzhou 510642, PR China  
Key Laboratory of Animal Vaccine Development, Ministry of Agriculture and Rural Affairs, Guangzhou 510642, PR China  
Key Laboratory of Zoonoses Prevention and Control of Guangdong Province, Guangzhou 510642, PR China

Junhai Zhu, Bo Li, Jinchao Xing

National and Regional Joint Engineering Laboratory for Medicament of Zoonoses Prevention and Control, South China Agricultural University, Guangzhou 510642, PR China  
Key Laboratory of Zoonoses Prevention and Control of Guangdong Province, Guangzhou 510642, PR China

Ming Liao\*, Wenbao Qi\*\*

National and Regional Joint Engineering Laboratory for Medicament of Zoonoses Prevention and Control, South China Agricultural University, Guangzhou 510642, PR China  
Key Laboratory of Zoonoses, Ministry of Agriculture and Rural Affairs, Guangzhou 510642, PR China

Guangdong Laboratory for Lingnan Modern Agriculture, Guangzhou 510642, PR China

Key Laboratory of Animal Vaccine Development, Ministry of Agriculture and Rural Affairs, Guangzhou 510642, PR China

Key Laboratory of Zoonoses Prevention and Control of Guangdong Province, Guangzhou 510642, PR China

\*Corresponding author at: National and Regional Joint Engineering Laboratory for Medicament of Zoonoses Prevention and Control, South China Agricultural University, Guangzhou 510642, PR China.

\*\*Corresponding author at: Key Laboratory of Zoonoses, Ministry of Agriculture and Rural Affairs, Guangzhou 510642, PR China.

E-mail addresses: [mliao@scau.edu.cn](mailto:mliao@scau.edu.cn) (M. Liao), [qiwenbao@scau.edu.cn](mailto:qiwenbao@scau.edu.cn) (W. Qi)

<sup>1</sup> These authors contribute equally to this work.

Accepted 26 February 2020

Available online 4 March 2020

<https://doi.org/10.1016/j.jinf.2020.02.025>

© 2020 The British Infection Association. Published by Elsevier Ltd. All rights reserved.

## Corona Virus Disease 2019, a growing threat to children?



Dear Editor,

Since the first case of Corona Virus Disease 2019 (COVID-19) was reported in Wuhan, China on December 8, 2019, the Severe Acute Respiratory Syndrome Coronavirus 2 (SARS-CoV-2) has spread rapidly to nationwide and 25 other countries<sup>1</sup>. By February 17, 2020, 72,436 cases and 1868 deaths have been confirmed on the Chinese mainland, with a fatality rate of 2.57%. Hubei had reported 59,989 cases of confirmed infections (including 42,752 in Wuhan) and 1789 deaths (including 1381 in Wuhan), with fatality rate of 2.98% in Hubei and 3.23% in Wuhan, respectively<sup>2</sup>.

In this Journal, Tang and colleagues have commented on the emergence of SARS-CoV-2 that infections in children and other vulnerable patients group are yet to be reported<sup>3</sup>. As diagnostic methods improving, 416 children under 10 years old have been reported in China<sup>4</sup>, in which 134 cases had the clinical records. Most of them had fever (76.1%) and viral pneumonia-like changes in chest imaging (70.4%). The main manifestations are fever, cough, followed by vomiting, diarrhea and other digestive system symptoms. Cases of neonatal infection were reported, one was diagnosed by pharyngeal swab nucleic acid test at 24 h after birth without any symptoms but low fever, CT scanning showed viral pneumonia (Fig. 1).

In Wuhan, the original place of COVID-19 outbreak, the first infected-child case was diagnosed on January 28, 2020, 8 days later than the first infected-child case reported city of Shenzhen, 1000 km far away from Wuhan. However, it does not mean that children in Wuhan were not suffering COVID-19 during the epidemic-period, nor the symptoms of infection occur later than the other areas. The possible causes for the delayed diagnosis of children in Wuhan are the overstrict diagnostic criteria and the shortage of testing reagent in the early stage. Afterwards, the number of children confirmed increased dramatically as the relaxation of the diagnostic criteria and the opening of nucleic acid tests for suspected cases of childhood on January 28, 2020, with 5 cases



**Fig. 1.** Newborn with COVID-19. A newborn whose mother was infected with COVID-19 showed low fever but no dyspnea after birth. The throat swab viral nucleic acid was positive 24 h later, and the lung CT showed viral pneumonia.

confirmed on the same day. Most children cases had mild symptoms, similar to other seasonal viral infections. Therefore, it has not attracted parents' enough attention. We noticed that most of the children were diagnosed during the epidemiological screening, with an exposure history to the familial clustering infection. It is a dangerous situation. The severity of children's infection has been ignored, furthermore, the asymptomatic infection in children may become a potential source of infection, which needs to be taken seriously.

Compared to infected adults, the condition of infected children is significantly milder, with faster recovery, shorter virus shedding time and better prognosis. By far, only 2 critical cases have been reported, of which one was a child of 7 months old with congenital heart disease. The other patient was 13 months old with bilateral hydronephrosis and calculus of left kidney. Both cases progressed rapidly to respiratory failure after onset, requiring support of invasive mechanical ventilation. It demonstrates that children with underlying diseases are tended to progress to severe and critical cases, so we should pay high attention to such group and strengthen supervision for them. In the laboratory tests part, blood cell count and procalcitonin (PCT) were basically normal, C-reactive protein (CRP) was normal or slightly increased. Some cases need two or even three tests to be confirmed. It suggests that although positive viral nucleic acid test is the "gold standard", clinical "false negative" children are also the potential source of infection. For clinical suspected cases, a continuous and repeated samples collection are need to improve the accuracy<sup>5</sup>.

Another urgent issue we are facing is how to perform antiviral therapy. Up to date, no effective anti-SARS-CoV-2 drug has been successfully confirmed in clinic practice. Since the outbreak of the SARS-CoV-2, interferons (IFN), Lopinavir/Ritonavir, Arbidol and even Oseltamivir have been recommended for clinical trials. IFN has been shown little effect in a variety of respiratory viral infections, the latter three are for influenza or HIV infection. Remdesivir is effective in a few cases of adult<sup>6</sup>, but there still lacks evidence-based clinical evidence for children. Since most children with respiratory viral infection merely have mild symptoms and can be self-healed, we consider that antiviral drugs should not be used routinely, unless in critical cases. The goals of treatment should be to alleviate symptoms and maintain the immune balance.

The epidemic characteristics of the COVID-19 in children are not yet clear, which poses a serious challenge to pediatric medical workers. Follow aspects should be pay special attention: Firstly, most children are asymptomatic or have mild symptoms. Even

if there are no symptoms, children from families with clustered infections should be screened for SARS-CoV-2 to eliminate potential sources of infection<sup>7</sup>. Secondly, to date, two critical cases in children have been identified. Both cases progressed rapidly. So, in epidemic season, children with underlying diseases should be protected by isolation as soon as possible. Thirdly, pregnant women infected in late pregnancy and newborns delivered by infected mothers. It is important to clarify the transmission route of mother-to-child vertical transmission or postnatal exposure in neonatal infection. According to our current limited data, in 21 pregnant women with confirmed infection in late pregnancy (8 cases were etiologically diagnosed, 13 cases were clinically diagnosed by chest CT), the amniotic fluid, placenta samples of mothers and pharyngeal swabs of newborns were collected<sup>8</sup>. The pharyngeal swabs were collected again the next day, all these samples showed negative results for nucleic acid test. The pharyngeal swab nucleic acid tests of 14 neonates were also negative on day 5 and 10 of their hospitalization. No evidence of mother-to-child vertical transmission was found. Finally, powerful broad-spectrum antibiotics and corticosteroids should be avoided<sup>9</sup>. In the period of COVID-19 outbreak, the incidence and fatality rate of severe cases in Hubei province, especially in Wuhan city, are significantly higher than that in other regions of China, which may be influenced by improper use of antibiotics and corticosteroids. Premature use and excessive coverage of antibiotics and corticosteroids may result in secondary infection<sup>10</sup>.

In summary, SARS-CoV-2 is generally susceptible to people of all ages. Most of the infections in children are familial clusters with mild clinical symptoms. Early isolation should be performed to protect children with underlying diseases, and it is necessary to enhance the protection during delivery and isolate the newborns immediately after delivery.

#### Declaration of Competing Interest

None reported.

#### Acknowledgment

We hereby acknowledge all health worker's efforts in Wuhan and other areas fighting against the COVID-19.



## References

1. Wu F., Zhao S., Yu B., Chen Y.M., Wang W., Song Z.G., et al. A new coronavirus associated with human respiratory disease in China. *Nature* 2020. doi:10.1038/s41586-020-2008-3.
2. National Health Commission of People's Republic of China: Daily briefing on novel coronavirus cases in China. [http://en.nhc.gov.cn/2020-02/18/c\\_76645.htm](http://en.nhc.gov.cn/2020-02/18/c_76645.htm).
3. Tang J.W., Tambyah P.A., Hui D.S.C.. Emergence of a novel coronavirus causing respiratory illness from Wuhan, China. *J Infect* 2020;80(3):350–71. doi:10.1016/j.jinf.2020.01.014.
4. Epidemiology Group Of Novel Coronavirus Pneumonia Emergency Response Mechanism Chinese center for disease control and prevention. epidemiological characteristics of novel coronavirus pneumonia. *Chin J Epidemiol* 2020;41(2):145–51.
5. World Health Organization: Home care for patients with suspected novel coronavirus (nCoV) infection presenting with mild symptoms and management of contacts. [https://www.who.int/internal-publications-detail/home-care-for-patients-with-suspected-novel-coronavirus-\(nCoV\)-infection-presenting-with-mild-symptoms-and-management-of-contacts](https://www.who.int/internal-publications-detail/home-care-for-patients-with-suspected-novel-coronavirus-(nCoV)-infection-presenting-with-mild-symptoms-and-management-of-contacts). 2020.
6. Holshue M.L., DeBolt C., Lindquist S., Lofy K.H., Wiesman J., Bruce H., et al. First case of 2019 novel coronavirus in the United States. *N Engl J Med* 2020 [Epub ahead of print]. doi:10.1056/NEJMoa2001191.
7. Shen K.L., Yang Y.H., Wang T.Y., Zhao D.C., Jiang Y., Jin R.M., et al. Diagnosis, treatment, and prevention of 2019 novel coronavirus infection in children: experts'consensus statement. *World J Pediatr* 2020. doi:10.1007/s12519-020-00343-7.
8. Chen H.J., Guo J.J., Wang C., Luo F., Yu X.C., Zhang W., et al. Clinical characteristics and intrauterine vertical transmission potential of COVID-19 infection in nine pregnant women: a retrospective review of medical records. *The Lancet* 2020. doi:10.1016/S0140-6736(20)30360-3.
9. Russell C.D., Millar J.E., Baillie J.K.. Clinical evidence does not support corticosteroid treatment for 2019-nCoV lung injury. *The Lancet* 2020;395(10223):473–5. doi:10.1016/S0140-6736(20)30317-2.
10. Wang D.W., Hu B., Hu C., Zhu F.F., Liu X., Zhang J., et al. Clinical characteristics of 138 hospitalized patients with 2019 novel coronavirus-infected pneumonia in Wuhan, china. *JAMA* 2020. doi:10.1001/jama.2020.1585.

Pu Yang<sup>1</sup>, Pin Liu<sup>1</sup>

Department of Pediatrics, Children's Digital Health and Data Center,  
Zhongnan Hospital of Wuhan University, Wuhan, China

Dan Li

East Ward of People's Hospital Attached to Wuhan University,  
Wuhan, China

Dongchi Zhao\*

Department of Pediatrics, Children's Digital Health and Data Center,  
Zhongnan Hospital of Wuhan University, Wuhan, China

\*Corresponding author.

E-mail address: zhao\_wh2004@hotmail.com (D. Zhao)

<sup>1</sup> Drs. Pu Yang and Pin Liu are co-first authors, contibuted  
equally to this article.

Accepted 26 February 2020  
Available online 3 March 2020

<https://doi.org/10.1016/j.jinf.2020.02.024>

© 2020 The British Infection Association. Published by Elsevier  
Ltd. All rights reserved.

## Disinfection Effect of Short-wave Ultraviolet Radiation(UV-C) on ASFV in Water



Dear Editor,

Recently, several reports in the Journal of Infection have highlighted the problem of African swine fever (ASF).<sup>1–3</sup> ASF caused by the African swine fever virus (ASFV), is a highly contagious hemorrhagic disease, affecting domestic pigs and wild boar, with a high morbidity and mortality.<sup>4</sup> In Asia, with the exception of Russia,

China was the first country to experience ASF and reported its first outbreak in August 2018.<sup>5</sup> Within a year, ASF quickly spread into all of the provinces in Mainland China. Small-scale pig farms with weak biosecurity systems account for a large proportion of China's pork production, which may be one reason for the rapid spread of ASF in China. In 2019, Mongolia reported the first ASF outbreak in January, followed by nine other Asian countries, including Vietnam, Cambodia, north Korea, Laos, Philippine, Myanmar, Russia, South Korea and Timor-Leste,<sup>3</sup> threatening neighboring unaffected countries and resulting in great biological and economic losses.

ASFV is very stable and can survive in meat and blood at room temperature for several months, which can be transmitted through several routes, including vehicle, personnel exchange or direct contact. Recently, an ASFV incursion in Romania has been reported in a large-scale, high-biosecurity farm. Contaminated water from the Danube River has been implicated in introducing ASF onto the ≈140,000-pig's farm. In addition, Dr. Niederwerder's study confirmed the high infectivity of ASFV Georgia 2007 through liquid by the oral route.<sup>6</sup> So, contaminated water is one of the biggest biosafety threats to farms, and inactivation of microorganisms in water is a vital way to prevent the spread of ASF. At present, for disinfecting drinking water, pig farms often use acidifiers to adjust the pH to reduce the adaptability of ASFV to the environment. However, the long-term use will cause gastric ulcers and other side effects in pigs. Apart from this, reverse osmosis methods can be used to purify groundwater, but the costs are very high; therefore, normal farms cannot afford it.

Ultraviolet-C (UVC) is a kind of ultraviolet light with a wavelength of 200–280 nm. The highest UV absorption peaks of DNA, RNA and nucleocapsid in pathogens are 254–257 nm. When pathogens absorb ultraviolet light, its DNA strands, nucleic acid and protein cross-links break. UVC light kills the biological activity of nucleic acid accordingly, causing causative agent to die. UVC light is known to have a strong bactericidal effect, inactivating a wide range of microorganisms such as viruses, bacteria, protozoa, fungi, yeast, and algae by forming pyridine dimers, a light product of genetic material.<sup>7</sup> UVC is a physical disinfection method, which plays an important role in water treatment.<sup>8</sup> With enough UVC radiation, pathogens in the water can be effectively inactivated in a short period of time.

To verify the efficacy of UVC light disinfection, we conducted the followings experiments. Firstly, the inactivation of ASFV by UVC was tested by controlling the dilution factor of ASFV and the treatment time in the UVC equipment. Ten-fold gradient dilutions were performed with 1 mL of ASFV stock solution. The diluted virus solution was aliquoted (200 μL) into quartz tubes. The virus solution diluted 100-fold was treated by UVC for 8 s, 30 s or 1 min; the virus solution diluted 1000-fold was treated by UVC for 8 s, 15 s, 30 s, 1 min or 2 min, and each time point was repeated twice. At the end of the treatment, the virus solution in the quartz tube was transferred to a 1.5-mL tube. The nucleic acid copy number was detected by real-time PCR (qPCR). Afterwards, the virus solution inactivated by the UVC in the quartz tube, was also cultured in PAMs. The presence or absence of ASFV biological activity was determined by testing whether ASFV grew in PAMs. The virus solution that had been diluted 1000-fold was aliquoted (200 μL) into quartz tubes. The quartz tubes containing virus solution were treated by UVC for 3 s, 8 s, 15 s or 30 s, and each time point was repeated four times. PAMs were seeded into three 24-well plates and cultured until the cell density reached 80%–90%, and the cells adhered and grew well. Four replicates were performed for each time point.

The results of our previous study showed that ASFV was inactivated when exposed to UVC at an intensity of 110–120 μw/cm<sup>2</sup> for 30 min. However, in this study, by increasing the number of UVC lamps in the water pipe, the intensity reached 3600 μw/cm<sup>2</sup>, and ASFV in water died within 3 s. The effect of UVC on nucleic acids

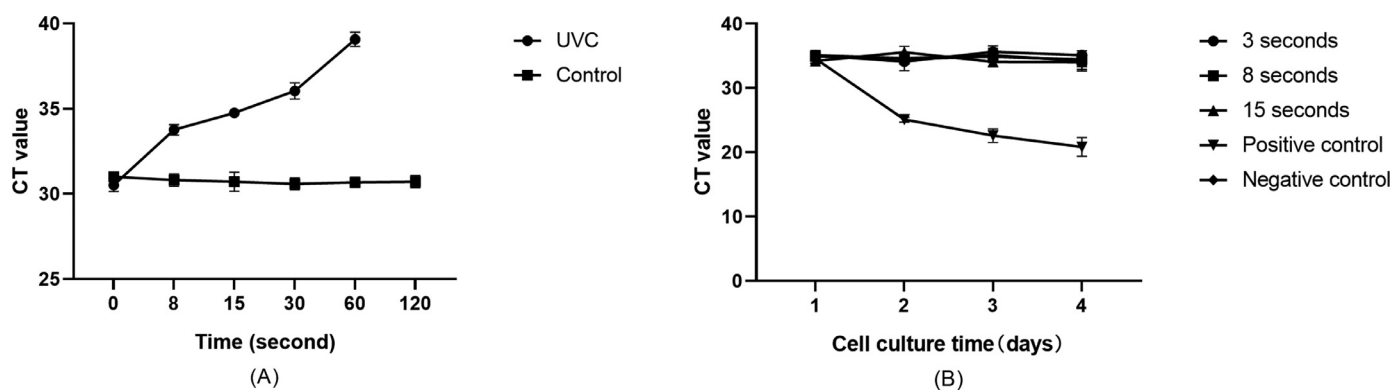


**Fig. 1.** Time-titre curve under UVC irradiation; (A) Detection of ASFV nucleic acid inactivation by UVC; (B) Characterization of the inactivation of the biological properties of ASFV by UVC. For the positive control, 50  $\mu$ l of untreated virus solution diluted 1000-fold and 450  $\mu$ l of 1640 culture medium were added to the cells. For the negative control, 500  $\mu$ l of 1640 culture medium was added to the cells.

is related to the irradiation time and intensity. However, when the treatment time was less than 1 min, the CT value of the sample was still positive, and only when the treatment time was more than 1 min was the sample test negative. The longer the irradiation time and the greater the intensity, the more serious is the damage to nucleic acid (Fig. 1(A)). None of the ASFV treated with UVC for 3 s, 8 s or 15 s could proliferate in PAMs (Fig. 1(B)). In winter, the disinfection effect of acidifiers and disinfectants on drinking water is greatly reduced, while UV is not affected. The effect of strong sunlight exposure on the infectivity of ASFV is also mainly affected by UV exposure.

In a word, for the current situation of widespread epidemic of African swine fever in China and the situation of escalating biosafety of farms. The use of UVC to sterilize drinking water for farm is of particular significance. It's worth noting that UVC in clear water was significantly more effective than in turbid water.<sup>9</sup> We carry out ultraviolet disinfection after water filtration, which can greatly improve the biosafety prevention and control of farms.

#### Declaration of Competing Interest

None.

#### Funding

This research was funded by the National Natural Science Foundation of China (31941004), the Key-Area Research and Development Program of Guangdong Province (2019B020211003), the Industry Technology System of Modern Agriculture Construction Fund (CARS-35).

#### References

- Ye C, Wu X, Chen T, Huang Q, Fang R, An T, et al. The updated analysis of African swine fever virus genomes: two novel genotypes are identified. *J Infect* 2020;**80**(2):232–54.
- Li X, Xiao K, Zhang Z, Yang J, Wang R, Shen X, et al. The recombination hot spots and genetic diversity of the genomes of African swine fever viruses. *J Infect* 2020;**80**(1):121–42.
- Lu G, Pan J, Zhang G. African swine fever virus in Asia: its rapid spread and potential threat to unaffected countries. *J Infect* 2020;**80**(3):350–71.
- Simulundu E, Chambaro HM, Sinkala Y, Kajihara M, Ogawa H, Mori A, et al. Co-circulation of multiple genotypes of African swine fever viruses among domestic pigs in Zambia (2013–2015). *Transbound Emerg Dis* 2018;**65**(1):114–22.
- Li X, Tian K. African swine fever in China. *Vet Rec* 2018;**183**:300–1.
- Niederwerder MC, Stoian AMM, Rowland RRR, Dritz SS, Petrovan V, Constance LA, et al. Infectious dose of African swine fever virus when consumed naturally in liquid or feed. *Emerging Infect Dis* 2019;**25**(5):891–7.
- Do-Kyun K, Dong-Hyun K. UVC LED irradiation effectively inactivates aerosolized viruses, bacteria, and fungi in a chamber-type air disinfection system. *Appl Environ Microbiol* 2018;**84**(17):e00918–44.

- Chevrefifils G, Caron É, Wright H, Sakamoto G, Payment P, Barbeau B, et al. UV dose required to achieve incremental log inactivation of bacteria, protozoa and viruses. *IUVA News* 2006;**8**:38–45.
- Bazyar Lakeh A.A., Kloas W., Jung R., Ariav R., Knopf K. Low frequency ultrasound and UV-C for elimination of pathogens in recirculating aquaculture systems. *Ultrason Sonochem* 2013;**20**(5):1211–16.

Runda Xu, Lang Gong, Heng Wang, Guihong Zhang\*  
Key Laboratory of Zoonosis Prevention and Control of Guangdong Province, College of Veterinary Medicine, South China Agricultural University, Guangzhou 510462, China  
Guangdong Laboratory for Lingnan Modern Agriculture, Guangzhou 510642, China  
African Swine Fever Regional Laboratory of China (Guangzhou), Guangzhou 510642, China  
Research Center for African Swine Fever Prevention and Control, South China Agricultural University, Guangzhou 510642, China

\*Corresponding author at: Key Laboratory of Zoonosis Prevention and Control of Guangdong Province, College of Veterinary Medicine, South China Agricultural University, Guangzhou 510462, China.

E-mail address: [guihongzh@scau.edu.cn](mailto:guihongzh@scau.edu.cn) (G. Zhang)

Accepted 20 February 2020  
Available online 2 March 2020

<https://doi.org/10.1016/j.jinf.2020.02.021>

© 2020 The British Infection Association. Published by Elsevier Ltd. All rights reserved.

#### Clinical features of atypical 2019 novel coronavirus pneumonia with an initially negative RT-PCR assay



#### Dear Editor,

Since end of December 2019, a cluster of patients with pneumonia of unknown origin was reported from Wuhan, Hubei province, China. They shared a connection with the Huanan South China Seafood Market in Wuhan, and now it has been confirmed that the disease is caused by a novel coronavirus (provisionally named 2019-nCoV). As of today (February 14, 2020), 63,935 cases have been confirmed in China. Currently, clinicians have found some atypical cases with positive chest CT findings may present with

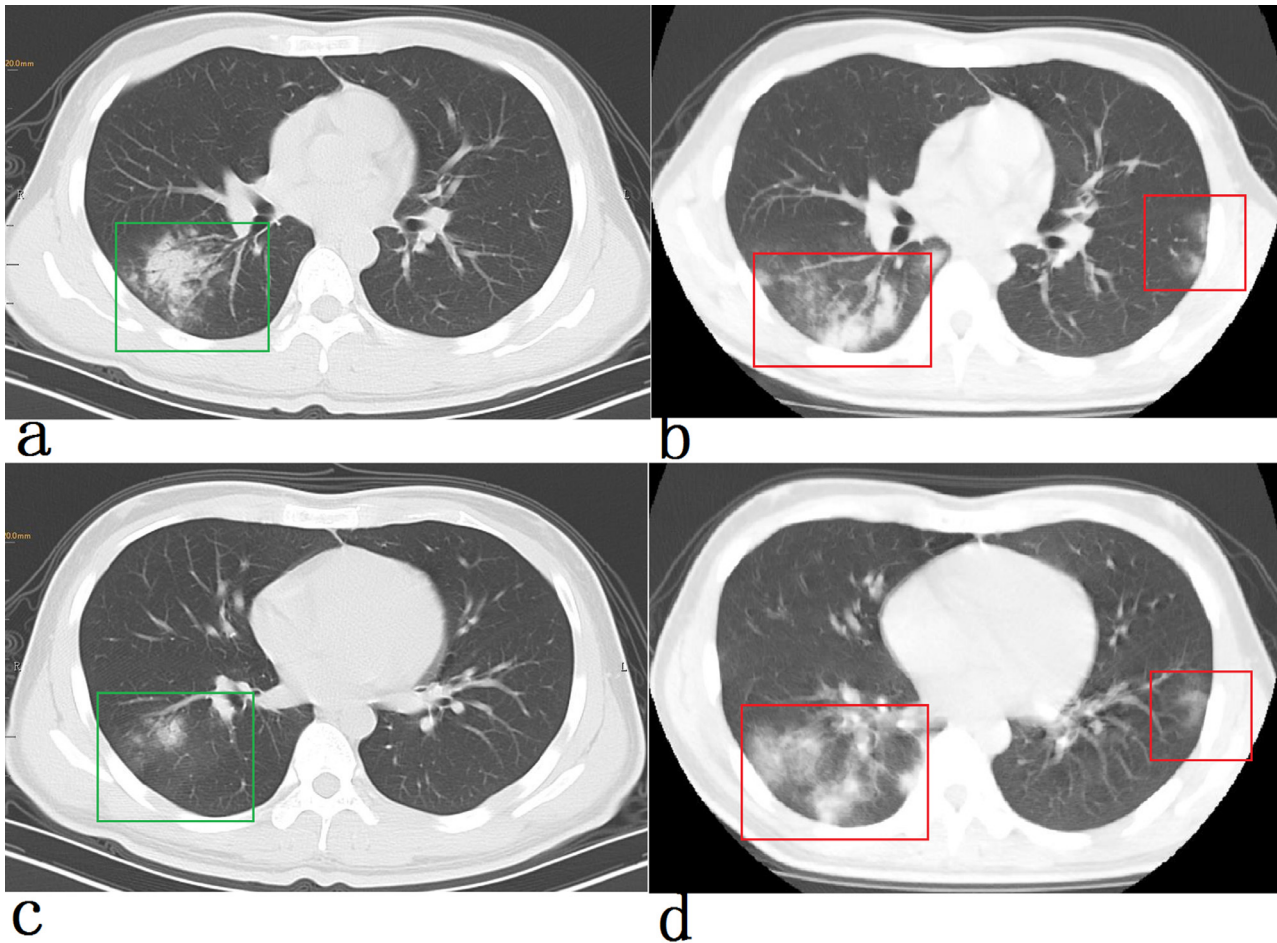


**Fig. 1.** Chest CT imaging of the patient (a, c) Chest CT scans obtained at admission show patchy high-density shadows on the dorsal segment of the right lower lobe (green boxes in a and c). (b, d) Image obtained 4 days after admission show large ground glass-like high-density shadows on the dorsal segment of the right lung, and patchy cloud-like high-density shadows and consolidation shadows on the left lung (red boxes in b and d).

negative results of RT-PCR for 2019-nCoV. The timely diagnosis, isolation and treatment of these patients will help control the further spread of 2019-nCoV.

We report a 58-year-old male who was admitted to the hospital with a 1-day history of fever, sore throat and fatigue 5 days after visiting Wuhan, China (the epicenter of the 2019 Novel Coronavirus Pneumonia outbreak).<sup>1</sup> Physical examination of the lungs at admission was normal. Laboratory studies demonstrated the white blood cell count ( $4.3 \times 10^9/L$ ) and blood procalcitonin level were also normal. The erythrocyte sedimentation rate was slightly increased at 23 mm/h (normal range, 0–20 mm/h). A swab test and chest CT scanning were performed. Chest CT images illustrated multiple patchy, cloud-like high-density shadows in the dorsal segment of the right lower lobe (Fig. 1a and c). Three real-time fluorescence polymerase chain reaction (RT-PCR) assay of the oropharyngeal swab specimens were negative for the 2019-nCoV nucleic acid.

A repeat chest CT performed 4 days after admission displayed that the range of patchy turbidity high-density shadows in the lower lobe of the right lung was significantly enlarged, and turbidity high-density shadows also appeared in the outer zone of the left lower lobe (Figure b & d). Finally, the fourth RT-PCR 2019-nCoV nucleic acid assay was positive.

Currently, clinicians have found some cases with positive chest CT findings may present with negative results of RT-PCR for 2019-nCoV. Although this patient's multiple specimen tests were negative, repeat chest CT showed a great progression of cloud-like high-

density shadows in both lungs compared to the previous chest CT. The imaging characteristics of 2019-nCoV pneumonia may be bifocal extra-zonal distribution, bilateral, multifocal<sup>2–3</sup>. With typical clinical presentation and a clear epidemiological history, 2019-nCoV infection may be strongly suspected when chest CT has the characteristics of viral pneumonia despite negative RT-PCR results. In these cases, repeat oropharyngeal swab testing and patient isolation should be carefully considered.

#### Contributors

W-DH obtained and analyzed the clinical data and made the figure. We all contributed to editing the figure, and writing and editing the manuscript. Written consent for publication was obtained from the patient.

#### Declaration of Competing Interests

None.

#### References

- Zhu N, Zhang D, Wang W, Li X, Yang B, Song J, et al. A novel coronavirus from patients with pneumonia in china, 2019. *N Engl J Med* 2020 Jan 24. doi:10.1056/NEJMoa2001017.
- Kanne Jeffrey P. Chest CT findings in 2019 novel coronavirus (2019-nCoV) infections from Wuhan, China: key points for the radiologist. *Radiology* 2020 Feb 04. doi:10.1148/radiol.2020200241.

3. Xie X., Zhong Z., Zhao W., Zheng C., Wang F., Liu J.. Chest CT for typical 2019-nCoV pneumonia: relationship to negative RT-PCR testing. *Radiology* 2020 Feb 12. doi:10.1148/radiol.2020200343.

Wendong Hao\*

Department of Respiratory and Critical Care Medicine, The Affiliated Hospital of Yan'an University, Yan'an 716099, Shaanxi, People's Republic of China

Department of Respiratory and Critical Care Medicine, The First Affiliated Hospital of Xi'an Jiaotong University, Xi'an 710061, Shaanxi province, People's Republic of China

Manxiang Li

Department of Respiratory and Critical Care Medicine, The First Affiliated Hospital of Xi'an Jiaotong University, Xi'an 710061, Shaanxi province, People's Republic of China

\*Corresponding author at: Department of Respiratory Medicine, The Affiliated Hospital of Yan'an University, No. 43 North Street, Baota District, Yan'an, Shaanxi Province, 716099, People's Republic of China.

E-mail address: [hwdokgood@hotmail.com](mailto:hwdokgood@hotmail.com) (W. Hao)

Accepted 17 February 2020

Available online 22 February 2020

<https://doi.org/10.1016/j.jinf.2020.02.008>

© 2020 The British Infection Association. Published by Elsevier Ltd. All rights reserved.

## Novel coronavirus (2019-nCoV) cases in Hong Kong and implications for further spread



Dear Editor,

Since Tang and colleagues commented on the current Wuhan novel coronavirus (2019-nCoV) outbreak four weeks ago,<sup>1</sup> the situation has worsened dramatically. As of today (1 February 2020), there have been an estimated 14,599 infected cases with a total of 305 deaths and 345 recovered involving 27 countries.<sup>2</sup> Online estimate of the case fatality rate is about 2% with a  $R_0$  (basic reproductive number) value of 3–4, indicating that every positive case may give rise to further 3–4 new cases. Nearly all confirmed cases (14,422, 98.8%) are in the mainland China, with most of the remaining cases in nearby countries or cities in East Asia (Japan, South Korea, Hong Kong, Taiwan, Macau), Southeast Asia (Thailand, Singapore, Malaysia, Vietnam) and Australia accounting for the majority of the remaining cases.<sup>2</sup> We would like to shed light on how the epidemic will develop in Hong Kong based on the characteristics of current cases in this region.

Hong Kong is a former British colony and a city situated in a small (426 m<sup>2</sup>iles) area officially designated as a Special Administrative Region (SAR) of the People's Republic of China. With a population of over 7.4 million, it has one of the highest population densities in the world. The geography of Hong Kong includes: (i) Hong Kong island, (ii) the Kowloon Peninsula and (iii) the New Territories which borders mainland China. It also consists of multiple islands, including the Lantau Island (the site of the Hong Kong International Airport). The busiest boundary control point with mainland China is in the New Territories at Lo Wu, where estimates from previous years indicate that around 239,000 passengers may be expected to cross daily during the Chinese New Year (CNY) period.<sup>3</sup> The closest city on the other side is Shenzhen within the Guangdong Province, and there are many people who

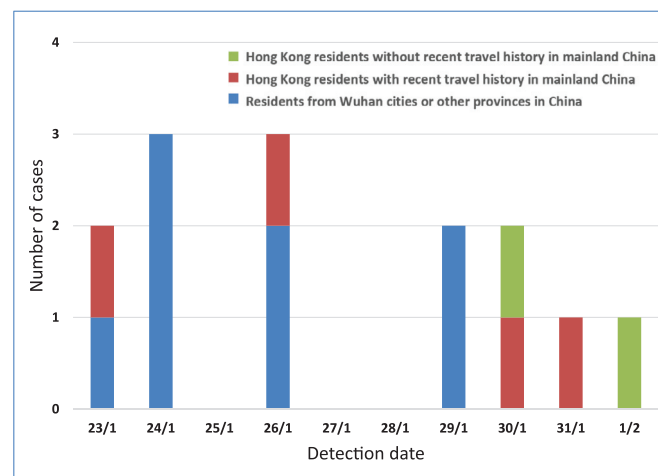


Fig. 1. Epidemic curve of Hong Kong 2019-nCoV cases. Note that for the Hong Kong residents without a travel history to mainland China (green bars), this applied to the 14 days prior to their symptom onset.

work in Hong Kong and live in Shenzhen, commuting across the border each day.

At the time of writing, 14 cases of the 2019-nCoV have been confirmed in Hong Kong and all are currently being managed at the designated infectious disease center - Princess Margaret Hospital (PMH). The first case was detected on 23 January 2020 and the most recent one was on the 1 February 2020. Most of these cases were residents from mainland China: Wuhan (7/14=50%) and Shenzhen (1/14=7.1%), visiting Hong Kong while the remaining 6 cases are Hong Kong citizens (Fig. 1).

At least two of these 14 cases had not travelled to the mainland China, including Wuhan, within the 14-day maximum incubation period of 2019-nCoV. They may therefore represent cases of inter-person transmission, having acquired their infections from infected individuals with such a travel history. Several cases of inter-person transmission have been reported in the other countries (including Japan, Germany and the United States).<sup>4–6</sup> This has also been reported in a family from Shenzhen who visited Wuhan (but not any wet markets) then infected one family member who had not travelled upon their return.<sup>7</sup> This Hong Kong cohort also consists of two husband-and-wife couples and a family of three (husband, wife and adult daughter), all of whom had a travel history to Wuhan.

The mean age of these 14 Hong Kong cases was 59.8 (S.D. 13.4) years and most (9/14=64.3%) were male. 12/14 (85.7%) cases presented with fever (including 5 with cough, 1 with blocked nose, 1 with muscle aches, and the remaining 2 afebrile cases exhibited coughing and shortness of breath). 10/14 (71.4%) cases presented to the Accident and Emergency departments in Hong Kong to seek care, 2/14 (14.3%) were intercepted by the Hong Kong Department of Health teams (using thermal imaging or temperature screening at border control points), and 2/14 (14.3%) developed symptoms and tested positive for 2019-nCoV during quarantine as a contact of a confirmed case. At present, 3/14 (21.4%) cases are in the intensive care unit (ICU) whereas the other 11 cases are clinically stable at PMH. An earlier report<sup>8</sup> on some of the earliest cases of 2019-nCoV infection also describes a higher proportion of cases to be male (30/41=73%), with a slightly higher proportion (13/41=32%) requiring ICU monitoring – though it is still yet possible that more Hong Kong cases may deteriorate and require ICU admission.

What do these early cases imply for Hong Kong? The period over which these cases were detected (23 January to 1 February 2020) includes the week before and the week after the CNY (starting from 25 January 2020). Does this suggest that this period represents the highest incidence of cases developing in Hong Kong be-

cause the highest intensity of population movement occurs over CNY, and that this may be expected to decrease once the celebrations are over? Not necessarily, we think, as many of the normal CNY activities in Hong Kong and mainland China were quite severely curtailed to limit the potential spread of this infection.<sup>9,10</sup> In which case, these incidence figures may represent more of the baseline rate of 2019-nCoV cases appearing in Hong Kong. Indeed, a closer look at Fig. 1 suggests that Hong Kong is already experiencing some degree of local inter-person transmission, as the earlier cases were associated with travel to Wuhan and other parts of mainland China, but the more recent cases involved no recent travel to these affected areas.

If this is the case, what can Hong Kong do? A previous study indicated that the mean daily contact rate for an individual in Hong Kong could be characterized as contacting 12–13 other people (both children and adults) spread over a total of nine-hour duration,<sup>11</sup> so presumably reducing the number of social contacts can reduce the risk of inter-person transmission. At present, all primary and secondary schools are closed in Hong Kong, and the universities are either postponing classes until March 2020 or are using distant/remote learning methods.<sup>12</sup> Another approach is to limit the number of potentially infected cases entering Hong Kong.<sup>13</sup> This strategy is controversial and our current modelling work is exploring its potential impact.

### Acknowledgments

This work has been partially supported by Research Fund for the Control of Infectious Diseases, Hong Kong (Number: INF-CUHK-1); General Research Fund (Number: 14112818); Health and Medical Research Fund (Ref: 18170312); Wellcome Trust (UK, 200861/Z/16/Z). The authors also thank Li Ka Shing Institute of Health Sciences for technical support.

### References

- Tang J.W., Tambyah P.A., Hui D.S.C. Emergence of a novel coronavirus causing respiratory illness from Wuhan, China. *J Infect* 2020 pii: S0163-4453(20)30038-4[Epub ahead of print]. doi:10.1016/j.jinf.2020.01.014.
- Wuhan coronavirus outbreak. 2 February 2020. <https://www.worldometers.info/coronavirus/>.
- Government of Hong Kong SAR. Cross-boundary passenger traffic estimation and arrangements for Lunar New Year festive period. 7 Feb 2018. <https://www.info.gov.hk/gia/general/201802/07/P2018020700291.htm>.
- The Japan Times. Japan reports first domestic transmission of coronavirus. 28 January 2020. <https://www.japantimes.co.jp/news/2020/01/28/national/japan-first-domestic-transmission-coronavirus/>.
- Global News. German man who never visited china catches coronavirus through human-to-human transmission. 28 January 2020. <https://globalnews.ca/news/6472303/german-coronavirus-human-to-human-transmission/>.
- CNN Health. First case of person-to-person transmission of Wuhan virus in the US confirmed. 30 January 2020. <https://edition.cnn.com/2020/01/30/health/coronavirus-illinois-person-to-person-cdc/index.html>.
- Chan J.F., Yuan S., Kok K.H., To K.K., Chu H., Yang J., et al. A familial cluster of pneumonia associated with the 2019 novel coronavirus indicating person-to-person transmission: a study of a family cluster. *Lancet* 2020 Jan 24 pii: S0140-6736(20)30154-9[Epub ahead of print]. doi:10.1016/S0140-6736(20)30154-9.
- Huang C., Wang Y., Li X., Ren L., Zhao J., Hu Y., et al. Clinical features of patients infected with 2019 novel coronavirus in Wuhan, China. *Lancet*. 2020 Jan 24 pii: S0140-6736(20)30183-5[Epub ahead of print]. doi:10.1016/S0140-6736(20)30183-5.
- Al Jazeera. Hong Kong cancels Chinese New Year celebrations. 18 January 2020. <https://www.aljazeera.com/news/2020/01/hong-kong-cancels-chinese-year-celebrations-200118140832768.html>.
- The Washington Post. Chinese cities cancel New Year celebrations, travel ban widens in effort to stop coronavirus outbreak. 24 January 2020. [https://www.washingtonpost.com/world/coronavirus-china-wuhan-latest/2020/01/23/2dc947a8-3d45-11ea-afe2-090eb37b60b1\\_story.html](https://www.washingtonpost.com/world/coronavirus-china-wuhan-latest/2020/01/23/2dc947a8-3d45-11ea-afe2-090eb37b60b1_story.html).
- Kwok K.O., Cowling B., Wei V., Riley S., Read J.M. Temporal variation of human encounters and the number of locations in which they occur: a longitudinal study of Hong Kong residents. *J R Soc Interface* 2018;15(138) pii: 20170838. doi:10.1098/rsif.2017.0838.
- South China Morning Post. Hong Kong schools, kindergartens closed until at least March 2 as coronavirus fears grow, three universities take similar action. 30 January 2020. <https://www.scmp.com/news/hong-kong/education/article/3048305/hong-kong-universities-suspend-classes-until-march-china>.
- South China Morning Post. China coronavirus: hong kong will ban anyone who has been to Hubei province from entering city, in response to mounting calls to tighten border checks. 26 January 2020. <https://www.scmp.com/news/hong-kong/health-environment/article/3047689/china-coronavirus-hong-kong-has-its-sixth-patient>.

Kin On Kwok\*

The Jockey Club School of Public Health and Primary Care, The Chinese University of Hong Kong, Hong Kong  
Stanley Ho Centre for Emerging Infectious Diseases, The Chinese University of Hong Kong, Shatin, Hong Kong, Special Administrative Region, China  
Shenzhen Research Institute of The Chinese University of Hong Kong, Shenzhen, China

Valerie Wong, Vivian Wan In Wei, Samuel Yeung Shan Wong  
The Jockey Club School of Public Health and Primary Care, The Chinese University of Hong Kong, Hong Kong

Julian Wei-Tze Tang\*\*

Clinical Microbiology, University Hospitals of Leicester NHS Trust, Leicester, UK  
Respiratory Sciences, University of Leicester, Leicester, United Kingdom

\*Corresponding author at: Room 419, School of Public Health, Prince of Wales Hospital, Shatin, Hong Kong, Special Administrative Region, China.

\*\*Corresponding author at: Clinical Microbiology, University Hospitals of Leicester NHS Trust, Level 5 Sandringham Building, Leicester Royal Infirmary, Infirmary Square, Leicester LE1 5WW, United Kingdom.

E-mail addresses: [kkokwok@cuhk.edu.hk](mailto:kkokwok@cuhk.edu.hk) (K.O. Kwok), [julian.tang@uhl-tr.nhs.uk](mailto:julian.tang@uhl-tr.nhs.uk) (J.W.-T. Tang)

Accepted 7 February 2020

Available online 22 February 2020

<https://doi.org/10.1016/j.jinf.2020.02.002>

© 2020 The British Infection Association. Published by Elsevier Ltd. All rights reserved.

### The continuous evolution and dissemination of 2019 novel human coronavirus



Dear Editor,

Recently, Wang and colleagues reported in this journal the new threat of novel SARS-like coronavirus in China.<sup>1</sup> During the last several decades, humans had been affected by six human coronaviruses (HCoV)—HCoV-NL63, HCoV-HKU1, HCoV-229E, HCoV-OC43, severe acute respiratory syndrome coronavirus (SARS-CoV), and Middle East respiratory syndrome coronavirus (MERS-CoV)—the last two of which caused severe respiratory symptoms and human death on a globe scale.<sup>2</sup> On December 2019, a human case in Wuhan, China infected with novel human coronavirus (HCoV) was first reported, who exhibited fever, difficulty with breathing, and invasive lesions in the lungs. This novel HCoV was subsequently designated as 2019-nCoV by World Health Organization (WHO). As of 4, February 2020, a total of 20,520 human cases (of which 426 fatal) of pneumonia infected with the 2019-nCoV had been demonstrated in all of the provinces of China (Fig. 1), with fatality rate of ~5% in Wuhan and ~0.8% in the rest of cities of China, respectively. Strikingly, the 2019-nCoV had caused family case clusters and sustained human-to-human transmission.<sup>3,4</sup> On January 30,

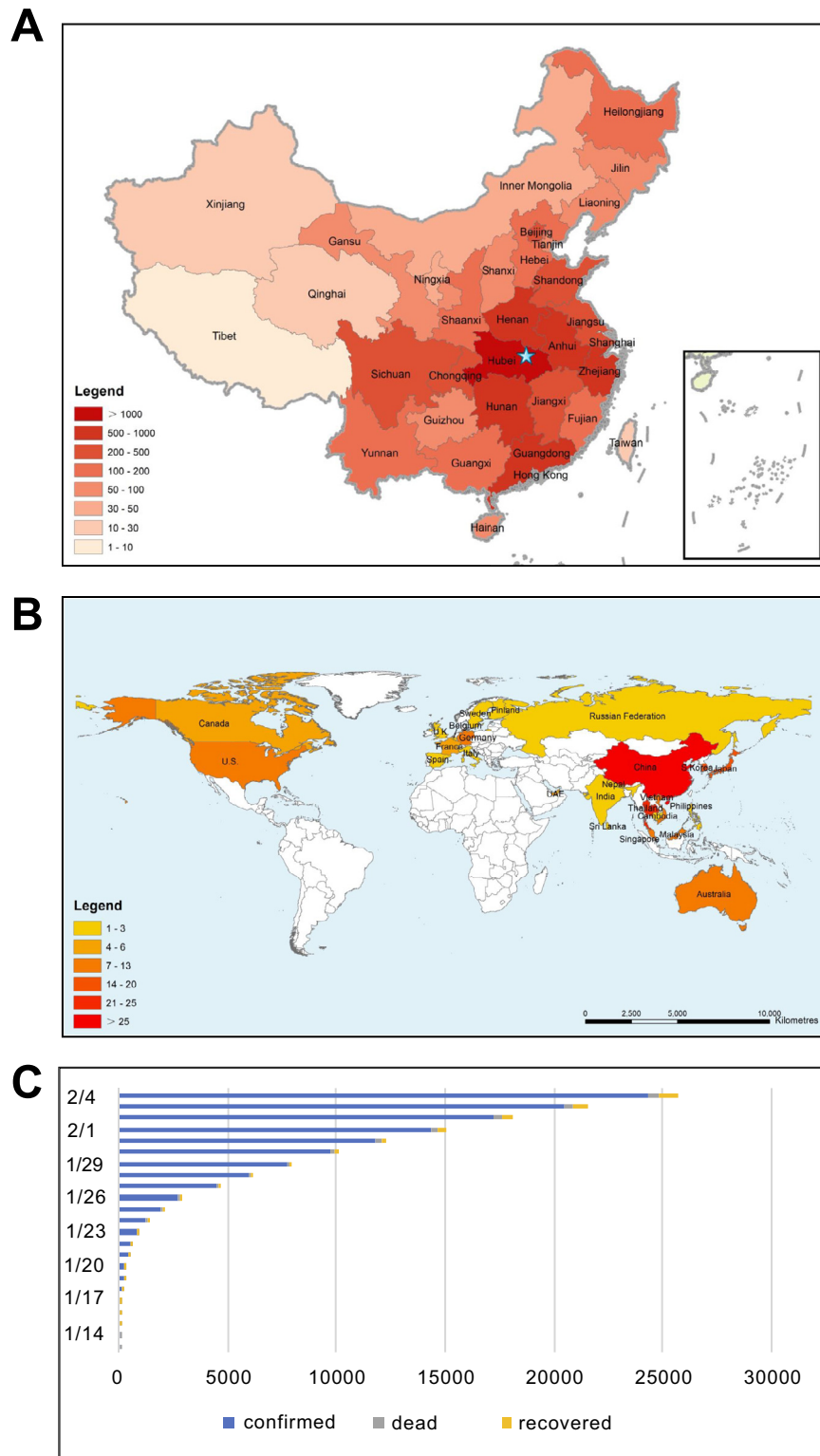


**Fig. 1. Geographic distribution of the 2019-nCoV and the number of human cases.** Geographic distribution of the 2019-nCoV in (A) China and (B) the world, respectively. The color of bar chart represents the number of human infection. The blue star represents the location of Wuhan, China. Data are available from the World Health Organization (<https://www.who.int>) and National Health and Family Planning Commission of the People's Republic of China (<http://www.nhfpc.gov.cn>). The map in the inset indicates islands in the South China Sea. The map was designed using ArcGIS Desktop 10.4 software (<http://www.esri.com/software/arcgis/arcgis-for-desktop/>). (C) The number of human cases by date are plotted, which shows a gradual increase over time. The blue bar chart represents the numbers of confirmed cases, and the gray bar chart represents the death toll, and the yellow bar chart represents the numbers of recovered cases.

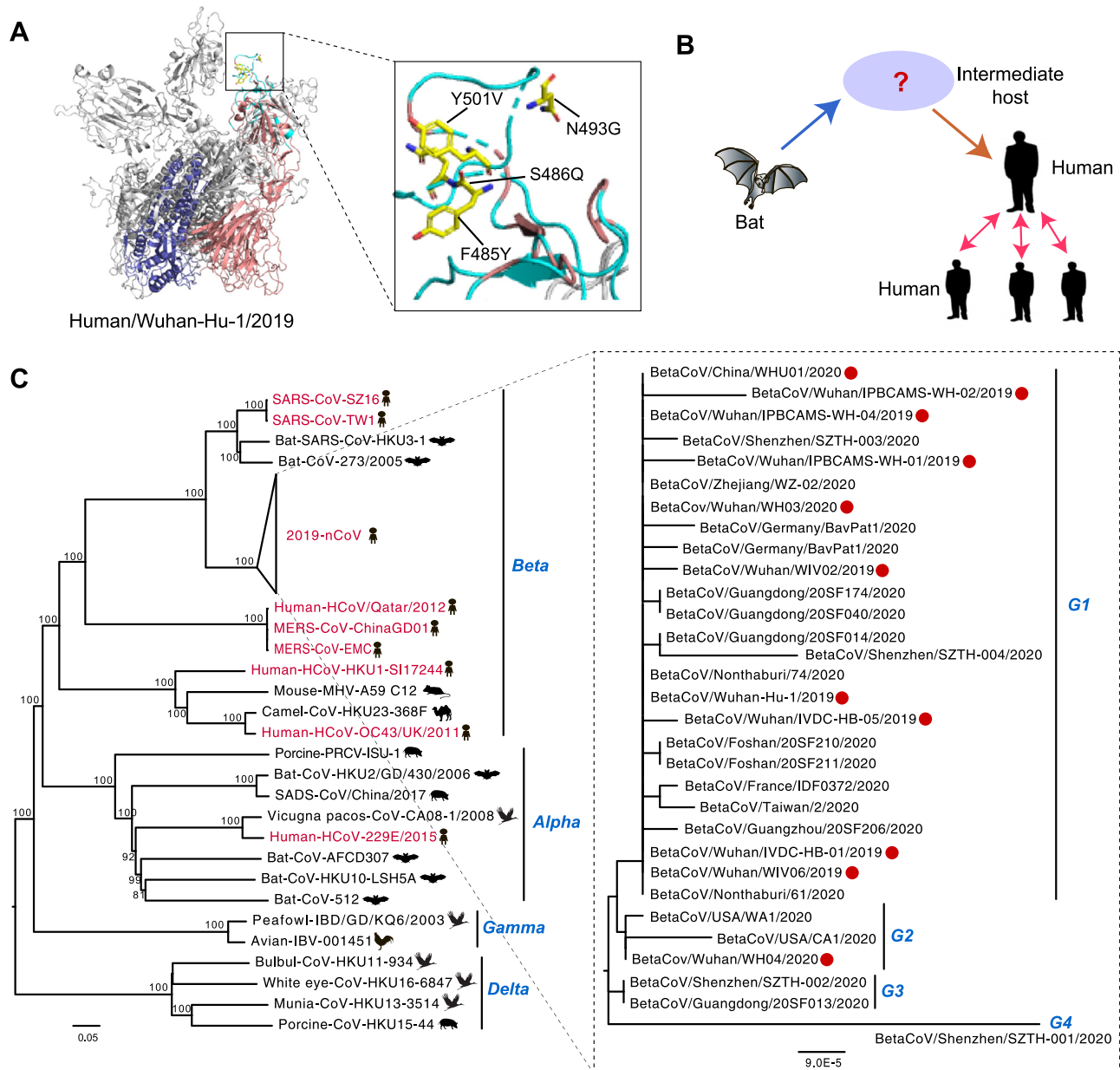


**Fig. 2. Evolutionary history of the 2019-nCoV.** (A) Structural analysis of envelope spike (S) protein of novel coronaviruses. The red and blue regions indicate the spike protein 1 and spike protein 2, respectively. The wathet blue region indicates the receptor binding region of 2019-nCoV. The correspondencing amino acids to the three-dimensional (3D) structure of the S protein were mapped using MacPymol (<http://www.pymol.org/>). (B) A simple model of 2019-nCoV origin inferred from phylogenetic tree and clinical feature of humans infected with the 2019-nCoV. (C) Maximum likelihood tree of the full-length genome of coronaviruses using MEGA 7 version. Red color indicates the human-origin coronaviruses, and red dot represents the isolates in Wuhan, China. The scale bar represents the number of nucleotide substitutions per site (subs/site).

2020, WHO declared the 2019-nCoV epidemic as a Public Health Emergency of International Concern (<https://www.who.int>), posing a new public health concern.

The emergence of novel 2019-nCoV highlights the necessity of tracing the origin of virus and the updated prevention and control systems in order to avert outbreaks. We found that the genomes of the novel 2019-nCoV were genetically closely related to beta SARS-related CoV (SARSr-CoV) circulating in China and had undergone genetic recombination with SARSr-CoV (Fig. 2 and Supplementary Figure S1–S3). The overall genome identity of the 2019-nCoV and SARSr-CoV was ranging from 82% to 89%. With rapid dissemination of the 2019-nCoV, the viruses had been transmitted rapidly in more than 25 countries, and a steep increase in human infection with the 2019-nCoV occurred in China (Fig. 1). To further explore the genetic evolution of the 2019-nCoV, phylogenetic relationships of 31 isolates examined in this study were explored and divided

into four genotypes, including G1, G2, G3, and G4. We found that 25 isolates clustered together and had been circulating in Thailand and multiple provinces (e.g. Taiwan, Guangdong, Zhejiang, and Hubei) of China, suggestive of the ongoing co-circulation of the viruses. The 2019-nCoV circulating in USA and Wuhan, China clustered into an independent cluster. However, interestingly, the SZTH-002, 20SF013, and SZTH-001 strains in Guangdong province were located at basal branch of the 2019-nCoV (Fig. 2), indicative of a single origin. The genetic diversity of RNA-dependent RNA polymerase of the 2019-nCoV was very small (Supplementary Figure S1). By contrast, the Spike (S) genes of some 2019-nCoV prevailing in Guangdong province were found at the root of the 2019-nCoV in Wuhan (Supplementary Figure S2). These findings indicated that the 2019-nCoV were infected from different regions in Wuhan and had been undergoing continuous evolution and dissemination in different regions. Compared with the rapid muta-

tion of the influenza A viruses, the degree of diversification of the 2019-nCoV was much smaller. Nevertheless, we cannot rule out if the 2019-nCoV continue evolving to become more transmissible and virulent in humans in the near future.

The S protein mediates receptor binding and membrane fusion, and of particular note, it is of great importance to determine host tropism and transmission capacity.<sup>5</sup> Zhou et al. demonstrated that the 2019-nCoV use the same cell entry receptor, ACE2, as SARS-CoV.<sup>6</sup> The receptor binding region of the 2019-nCoV was more similar to that of SARS-CoV; however, we found that four amino acid substitutions in the receptor binding region of the 2019-nCoV, including S486Q, F485Y, N493G, and Y501V substitutions (2019-nCoV numbering), were different from that of SARS-CoV (Fig. 2), which might affect the receptor binding ability.

Bats provide a rich “gene pool” for interspecies exchange of genetic fragments of CoV.<sup>7</sup> Continuous surveillance in bats provide us a clue to the correlation between the 2019-nCoV and the animal origin CoV. Despite the shared cluster between the 2019-nCoV and bat SARSr-CoV, we cannot infer that the reservoir of the 2019-nCoV was originated from bats. Most of the patients infected with novel 2019-nCoV had a history to the seafood and live animal markets, and the vendor used to sale wild animal species, including marmot, snake, leopard cat, bamboo rat, badger, and hedgehog in Huanan seafood wholesale market (Supplementary Figure S4), all of which were susceptible to the novel CoV in nature, indicating that it remains likely there was intermediate hosts in the transmission cascade from bats to humans (Fig. 2). However, a question of a public health interest is which intermediate hosts harbor the 2019-nCoV that could infect humans, which should be examined in greater detail. Recently, the continuous interspecies transmission events of CoV occurred, including the emergence of MERS-CoV from camels to humans and swine acute diarrhoea syndrome CoV from bat to swine, posing serious threats to public health.<sup>8,9</sup> With the tradition of feeding wild animals for food or use in traditional medicine in China, wild birds, mammals, and reptiles carrying the novel zoonotic viruses flowed frequently in trading center, which had considerable potential to transmit to humans of emerging viruses.

In 2018, China had participated a Global Virome Project to identify unknown viruses from wildlife to better prepare for the epidemics of infectious diseases in humans.<sup>10</sup> With multiple species of CoV circulating in different animal species that could be transmitted to humans, no one knows when or where the next outbreak will occur. Nevertheless, decreasing the risk for the spread of novel viruses including reducing contact among humans and wild animal species and stopping novel viruses at their origins is urgently needed. We call upon wildlife biologists, ecologists, doctors, and veterinarians should promote exchange and share data across disciplines as a mean to minimize the potential for pandemics of the 2019-nCoV.

#### Declaration of Competing Interest

All authors have no potential conflicts of interest to disclose.

#### Acknowledgement

We sincerely thank the authors of the human 2019 coronavirus from GISAID EpiFlu™ Database. This work was supported by the National Natural Science Foundation of China (31941014, 31830097, 31672586), Key Research and Development Program of Guangdong Province (2019B020218004), Earmarked Fund for China Agriculture Research System (CARS-41-G16), Guangdong Province Universities and Colleges Pearl River Scholar Funded Scheme (2018, Wenbao Qi), and Young Scholars of Yangtze River Scholar Professor Program (2019, Wenbao Qi).

#### Supplementary materials

Supplementary material associated with this article can be found, in the online version, at doi: [10.1016/j.jinf.2020.02.001](https://doi.org/10.1016/j.jinf.2020.02.001).

#### References

1. Wang R., Zhang X., Irwin D.M., Shen Y. Emergence of SARS-like Coronavirus poses new challenge in China. *J Infect* 2020. doi:[10.1016/j.jinf.2020.01.017](https://doi.org/10.1016/j.jinf.2020.01.017).
2. Su S., Wong G., Shi W., et al. Epidemiology, genetic recombination, and pathogenesis of coronaviruses. *Trends Microbiol* 2016;24(6):490–502.
3. Huang C., Wang Y., Li X., Ren L., Zhao J., Hu Y., et al. Clinical features of patients infected with 2019 novel coronavirus in Wuhan, China. *Lancet* 2020. doi:[10.1016/S0140-6736\(20\)30183-5](https://doi.org/10.1016/S0140-6736(20)30183-5).
4. Chan J.F., Yuan S., Kok K.H., To K.K., Chu H., Yang J., et al. A familial cluster of pneumonia associated with the 2019 novel coronavirus indicating person-to-person transmission: a study of a family cluster. *Lancet* 2020. doi:[10.1016/S0140-6736\(20\)30154-9](https://doi.org/10.1016/S0140-6736(20)30154-9).
5. Lu G., Wang Q., Gao G.F. Bat-to-human: spike features determining ‘host jump’ of coronaviruses SARS-CoV, MERS-CoV, and beyond. *Trends Microbiol* 2015;23:468–78.
6. Zhou P., Yang X., Wang X., Hu B., Zhang L., Zhang W., et al. A pneumonia outbreak associated with a new coronavirus of probable bat origin. *Nature* 2020. doi:[10.1038/s41586-020-2012-7](https://doi.org/10.1038/s41586-020-2012-7).
7. Hu B., Zeng L., Yang X., Ge X., Zhang W., Li B., et al. Discovery of a rich gene pool of bat SARS-related coronaviruses provides new insights into the origin of Sars coronavirus. *Plos Pathog* 2017;13(11):e1006698.
8. Shen X., Sabir J.S.M., Irwin D.M., Shen Y. Vaccine against Middle East respiratory syndrome coronavirus. *Lancet Infect Dis* 2019;19(10):1053–4.
9. Zhou P., Fan H., Lan T., Yang X., Shi W., Zhang W., et al. Fatal swine acute diarrhoea syndrome caused by an HKU2-related coronavirus of bat origin. *Nature* 2018;556(7700):255–8.
10. Carroll D., Daszak P., Wolfe N.D., Gao G.F., Morzaria S., Pablos-Méndez A., et al. The global virome project. *Science* 2018;359(6378):872–4.

Jiahao Zhang<sup>1</sup>, Kaixiong Ma<sup>1</sup>, Huanan Li  
National and Regional Joint Engineering Laboratory for Medicament  
of Zoonoses Prevention and Control, South China Agricultural  
University, Guangzhou 510642, PR China  
Key Laboratory of Zoonoses Prevention and Control of Guangdong  
Province, Guangzhou 510642, PR China

Ming Liao\*, Wenbao Qi\*  
National and Regional Joint Engineering Laboratory for Medicament  
of Zoonoses Prevention and Control, South China Agricultural  
University, Guangzhou 510642, PR China  
Key Laboratory of Zoonoses, Ministry of Agriculture and Rural  
Affairs, Guangzhou 510642, PR China  
Guangdong Laboratory for Lingnan Modern Agriculture, Guangzhou  
510642, PR China  
Key Laboratory of Animal Vaccine Development, Ministry of  
Agriculture and Rural Affairs, Guangzhou 510642, PR China  
Key Laboratory of Zoonoses Prevention and Control of Guangdong  
Province, Guangzhou 510642, PR China

\*Corresponding authors at: National and Regional Joint Engineering  
Laboratory for Medicament of Zoonoses Prevention and Control,  
South China Agricultural University, Guangzhou 510642, PR  
China.

E-mail addresses: [mliao@scau.edu.cn](mailto:mliao@scau.edu.cn) (M. Liao),  
[qiwenbao@scau.edu.cn](mailto:qiwenbao@scau.edu.cn) (W. Qi)

<sup>1</sup> These authors contribute equally to this work.  
Accepted 7 February 2020  
Available online 22 February 2020

<https://doi.org/10.1016/j.jinf.2020.02.001>

© 2020 The British Infection Association. Published by Elsevier  
Ltd. All rights reserved.